DANMARKS OG GRØNLANDS GEOLOGISKE UNDERSØGELSE RAPPORT 2003/106

Chalk structure maps of the central and eastern North Sea

Top and base chalk in depth and time

O. V. Vejbæk, T. Bidstrup, P. Britze, M. Erlstrøm,
E. S. Rasmussen and U. Sivhed

GEUS

DANMARKS OG GRØNLANDS GEOLOGISKE UNDERSØGELSE RAPPORT 2003/106

Chalk structure maps of the central and eastern North Sea

Top and base chalk in depth and time

O. V. Vejbæk, T. Bidstrup, P. Britze, M. Erlstrøm,
E. S. Rasmussen and U. Sivhed

GEOLOGICAL SURVEY OF DENMARK AND GREENLAND
MINISTRY OF THE ENVIRONMENT

G E U S

Contents

1 Introduction

This report presents new detailed maps of the top and base of the Chalk Group for the central and eastern North Sea (Fig. 1). Mapping scale is 1:1170000 with a contour interval of 50 msec and 50 m for time and depth maps respectively. Resulting depth converted maps of the top chalk, base chalk and chalk isopach are given as enclosures whereas time and velocity maps are given as illustration in 1:6,900,000. Underlying grids have gridspacings of $500 \cdot 500m$ and 1.68 million grid cells. Maps are all presented in the UTM projection in zone 32 (central meridian 9°E) using the Hayford 1909 ellipsoid. About three quarters of the mapped area are taken from GEUS in-house mapping campaigns, either done previously or specifically for this project. The remainder is modified from various published maps. These other sources are in many cases only available in projections other than UTM zone 32 and various conversion techniques therefore had to be applied (see appendix).

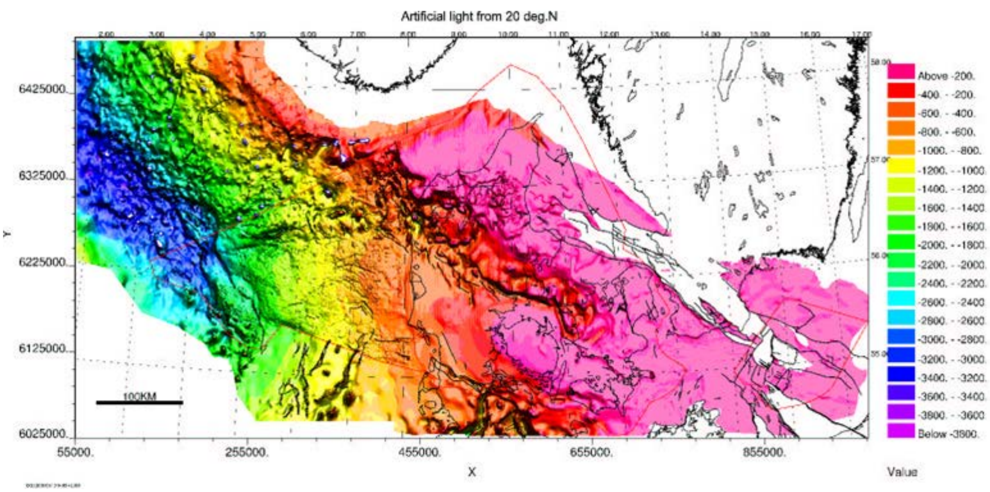

Figure 1: Top Chalk time structure map. Illuminated from the north-east.

The comprehensive data base includes Shallow, 2D and 3D seismic data as well as published maps in authoritative projections (e.g. Baldschuhn *et al.* 2001; Britze *et al.* 1995). Control on the mapping is provided by industrial wells and numerous onshore water wells. The mapped stratigraphic interval comprises the Chalk Group and equivalent formations in the stratigraphic interval (and including) Cenomanian to Danian. The summarized lithostratigraphy for the mapped interval is shown in Fig. 3. Although limestone and chalk dominates the mapped interval, other lithologies are also present. Notable exceptions are the clayey intercalations of the Shetland Group in the northernmost part of the mapped area, and the siliciclastic sand members of the Arnager Greensand, and the Lunda and Hansa members in the easternmost part of the area. The Lunda Member even comprise clean quartz sands of several hundred meter thickness (Erlström 1990; 1994). One omitted unit from the scheme in Fig. 3 is the Bavnodde Greensand that is exposed on Bornholm and which is time equivalent with the older parts of the Lunda Member. Carbonates also encompass the Danian bryozoan and coral limestones found in the eastern parts (e.g. Stevns Klint, Fakse Limestone Quarry, etc.), and many further local names exist (e.g. Surlyk 1982). The northeastern limit of the Chalk Group is everywhere determined by Neogene erosion. Map limits to the west and south are arbitrary, but are also determined by lack of data.

In the following section brief descriptions of the maps are given. Location names used in these description may be found on Fig. 2 and in Table 4. This is followed by an extensive account of the applied depth conversion techniques.

Abbreviation	Full name	Abbreviation	Full name
ASB	Arnager-Sose Block	KoF	Koszalin Fault
BBl	Bornholm Block	KoG	Kolobrzeg Graben
BF	Børglum Fault	KRAF	Kullen Ringsjön Andrarum Fault
BT	Brande Trough	KrFZ	Krebs Fault Zone
ChH	Christiansø High	KHo	Kullen Horst
CSF	Coffee Soil Fault	LFBC	Lista Fault Block Complex
CST	Colonus Shale Trough	MaH	Mandal High
DaBl	Darlowo Block	MH	Mads High
EB	Egersund Basin	MNH	Mid North Sea High
EG	Else Graben	MøH	Møn High
ENBl	East North Sea Block	ORB	Outer Rough Basin
EH	Eigerøy Horst	RB	Rott Basin
FaB	Farsund Basin	RFZ	Romele Fault Zone
FG	Feda Graben	RiH	Ringe High
FT	Fjerritslev T-rough	RoR	Romele Ridge
GFZ	Gyda Fault Zone	RT	Risebæk Trough
GG	Gertrud Graben	SB	Søgne Basin
GHF	Grenå- Helsingborg Fault	ScH	Schillergrund High
GlG	Glückstadt Graben	SDP	Salt Dome Province
GlBl	Glamsbjerg Block	SkG	Skagerrak Graben
GNB	Grensen Nose Basin	SkP	Skurup Platform
GrBl	Grindsted Block	ST	Svaneke Trough
GrG	Gryfice Graben	StP	Stavanger Platform
GrW	Grimmener Wall	SvF	Svedala Fault
GuT	Gudhjem Trough	SvH	Sørvestlandet High
HBl	Holmsland Block	SæF	Sæby Fault
HBB	Hanö Bay Basin	TEG	Tail End Graben
HeT	Helgoland Trough	UsBl	Ustka Block
HFZ	Hummer Fault Zone	VFZ	Varde Fault Zone
HiG	Himmerland Graben	VG	Varnes Graben
HF	Holmsland Fault	VT	Vomb Trough
HG	Horn Graben	WSBl	West Schleswig Block
HöG	Höllvik Graben	YRH	Ystad - Rønne High
IH	Inge High		
KFZ	Krabbe Fault Zone		

Table 4: Abbreviations of structural names shown on Fig. 2.

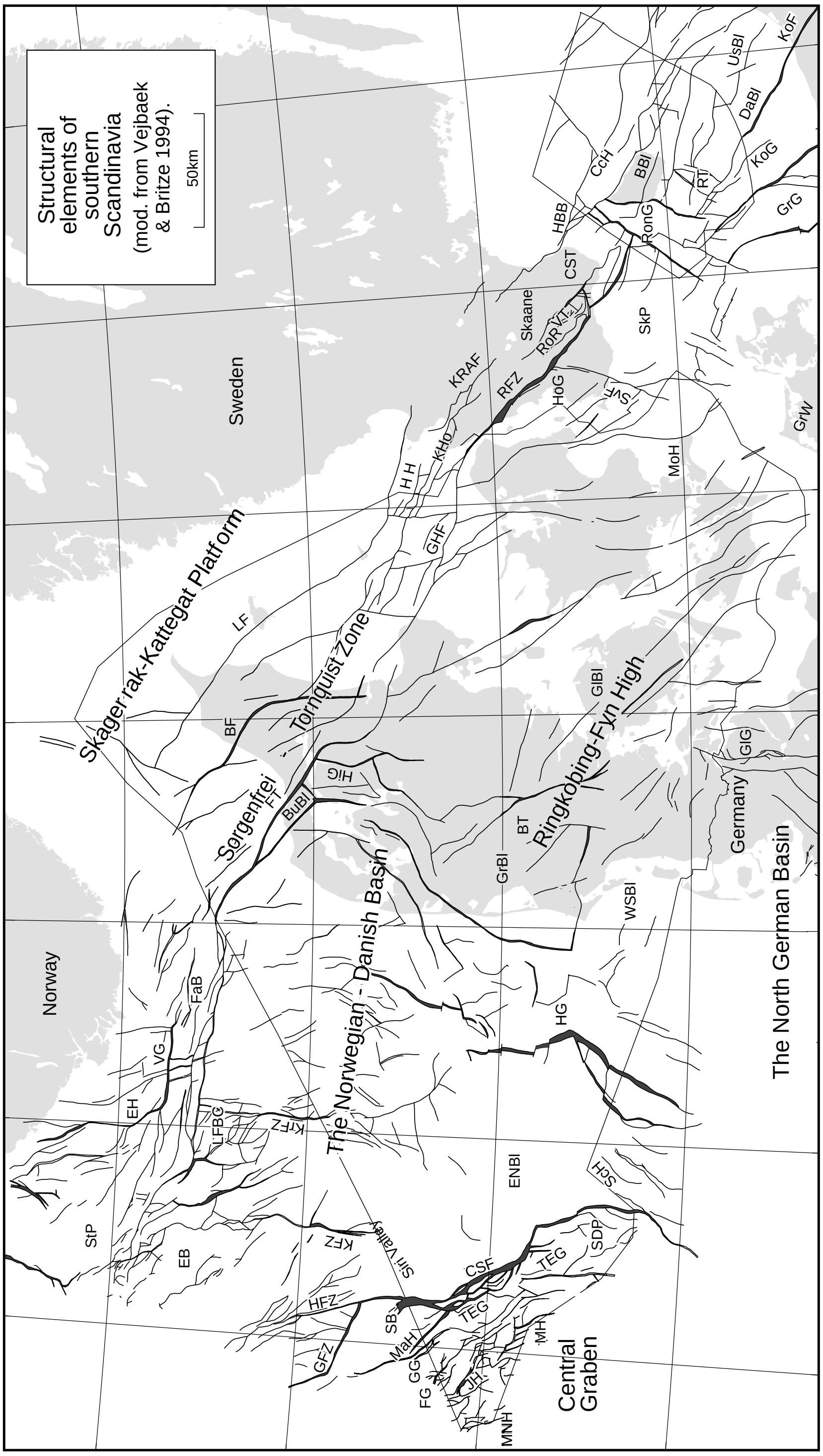

Figure 2: General structural elements of the study area showing simplified Top pre-Zechstein fault patterns (mod. from Vejbæk and Britze 1994).

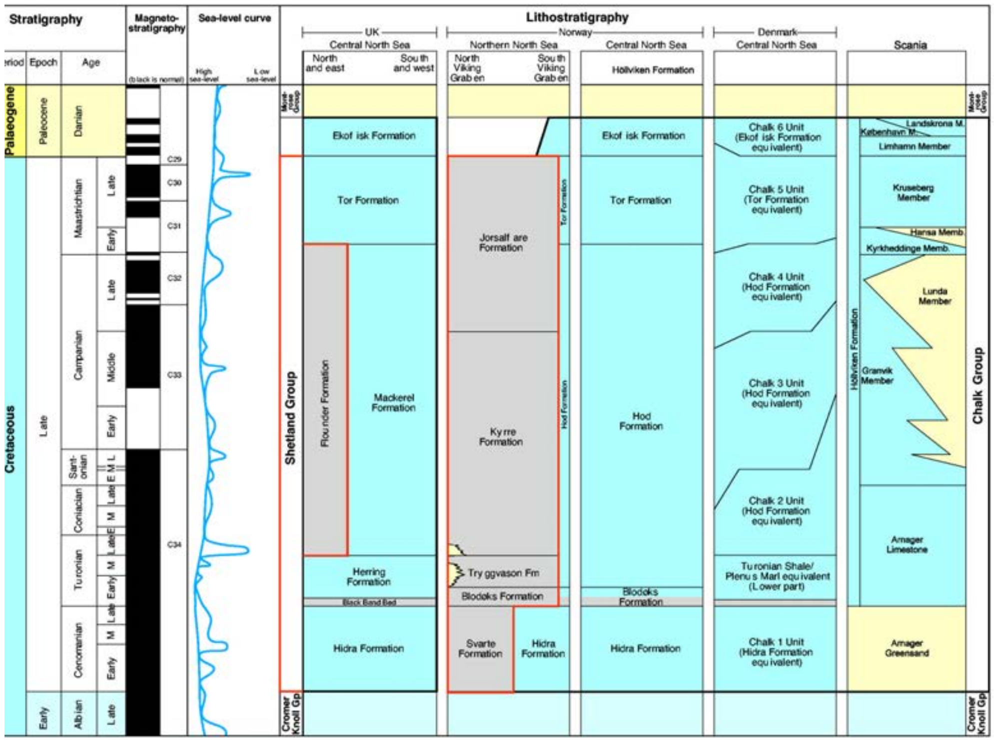

Figure 3: Lithostratigraphic correlation for the Upper Cretaceous - Danian succession mapped in this report. Top and Base Chalk maps correspond to top and base of the light blue/grey units (mod. from Surlyk *et al.* 2003; Sivhed *et al.* 1999 and based on Deegan and Scull 1977; Isaksen and Tonstad 1989; Johnson and Lott 1993).

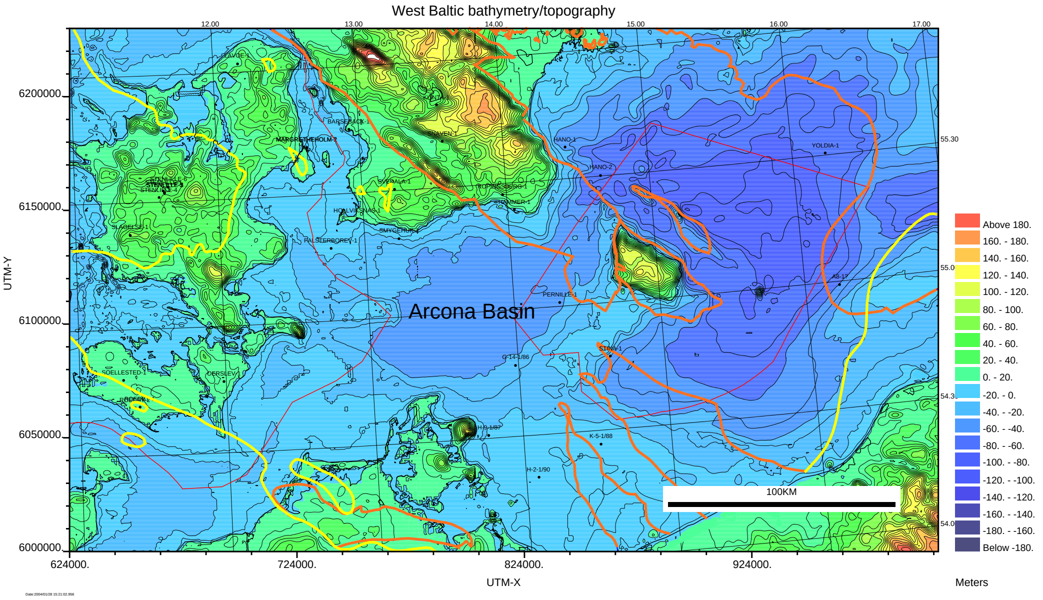

Figure 4: Topography and bathymetry in the western Baltic. Thich red lines show extent of Chalk Group deposits. Yellow lines show extent of post chalk Palaeogene deposits. Contour interval is 10m.

2 Top Chalk map

Major sources for this map are the earlier GEUS maps covering the Central Graben (Britze *et al.* 1995), and north - central Jylland (Ter-Borch 1991; Britze *et al.* 1991). Unpublished earlier mapping has contributed to the major part of the Norwegian sector where mapping detail is determined by a 1 km gridspacing. However, north of the 58° parallel and likewise in the British North Sea sector, only grids from the Millennium Atlas (Surlyk *et al.* 2003) have been available with a gridspacing of 2 km. The entire German sector has been obtained by digitization of the Gauss Krüger projected maps published by Baldschuhn *et al.* (2003). These maps are only available in depth converted version, so they had to be converted back to time before merging with the northern areas, as compilation is done in the reflection time domain.

The velocity field for this operation is a model based extrapolation from the Danish sector because well velocity data has not been available for the German sector (see section on depth conversion).

The reflection time map is therefore more uncertain than the depth map in the German sector. New mapping specifically for this project has been undertaken in South Jylland, in parts of the Central Graben (based on 3D data) and in the North Sea between the Central Graben and Jylland.

In the Skagerrak area, the Top Chalk has been supplemented with published maps (NGU 96.138; Jensen 1998).

The eastern parts of the Top Chalk maps are shown with a dot raster that signifies erosion or direct superposition by Quaternary deposits (Fig. 6). These areas are compiled on the basis of water wells and shallow seismic surveys offshore (e.g. Binzer and Stockmarr 1994; Kramarskiej 1999; Køgler and Larsen 1979; Lemke 2000; Sivhed *et al.* 1999; Stenestad 1976; Ter-Borch 1991). In some areas like in the Arkona Basin, no shallow seismic surveys have been found, so there the bathymetry (Kramarskiej 1999; Seifert and Kayser 1995) plus an estimate on the Quaternary thickness has provided an estimate on the Top Chalk depth (Figs 4, 5).

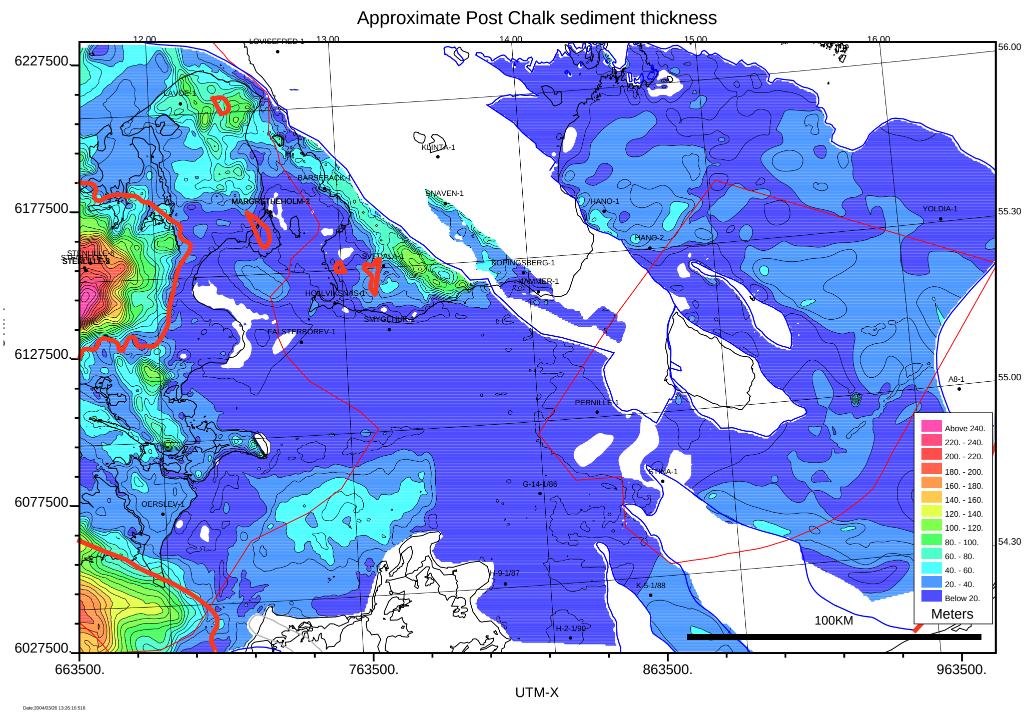

Figure 5: Approximate thickness of Postdanian Cenozoic deposits. In most of the area, it is equivalent to the Quaternary except for minor areas outlined with thick red lines. Contour interval is 10m.

In the areas with only Quaternary overburden, the primary data sources have only provided depth and not reflection time. Due to lack of data and large uncertainty in velocity mapping, this is considered futile and a velocity of 2 km/sec has been assumed such that depths in meters and reflection time has the same value. Within the rasterized area, in the eastern part of the map, small areas without raster signature indicate outliers of Seelandian and/or other Palaeogene deposits. This is proven in the Copenhagen (and North Sjælland) area (e.g. Stenestad 1976), in Scania (Sivhed *et al.* 1999), in the Polish offshore (Kramarskiej 1999), and onshore eastern Germany (Best *et al.* 2000). These and immediately adjacent areas therefore have almost complete Chalk successions in spite of the large hiatus between Palaeogene and Quaternary deposits and Neogene erosion has not removed large amounts of the Chalk although circumstantial evidence suggests that considerable thicknesses of chalk overburden has been removed by erosion (e.g. Japsen 1993; 2000; Japsen and Bidstrup 1999).

The areas with preserved post chalk Palaeogene deposits are characteristically located adjacent to conspicuous inversion zones as the Sorgenfrei Tornquist zone, the Kolobrzeg and Gryfice grabens and the Grimmener Wall. Within these inversion zones, however, the chalk succession is far from complete, and is even missing in major parts.

In Norwegian waters, however, deep angular truncation characterizes the area where Neogene erosion has occurred (see section on thickness maps). A general thickness increase of the Chalk in a northeasterly direction is seen in the Norwegian offshore until the area where Neogene erosion has occurred. Similar thickness increases are seen towards the established inversion zone of the Sorgenfrei - Tornquist Zone. It may be surmised that the northeasterly thickness increase in Norwegian waters may constitute the same phenomenon; namely depocentres at the flanks of inversion zones. It may thus be further surmised, that an inversion zone could have been present in the southwestern coastal areas of Norway, but is now impossible to recognize due to total removal of Phanerozoic sediments by Neogene erosion.

Notable features are erosion channels/valleys: The broad Siri Valley originates at a large salt dome northeast of the Norwegian well 10/11-1, and runs southwestwards along the Danish - Norwegian border to the edge of the Central Graben (at the Elna-1 well). Another narrow valley runs all the way from the Slagelse-1 well, south of the Horsens-1 and Vinding-1 wells and westwards passing the Ibenholt-1 well to the Central Graben. This valley is closely associated with a series of faults that generally detach in the underlying Zechstein salt approximately at the transition from marginal carbonates to basinal salt along the north edge of the Ringkøbing - Fyn High (e.g. Vejbæk 1997). Similar salt related detachments are developed in the Tønder Trough located near the Danish - German border onshore Denmark.

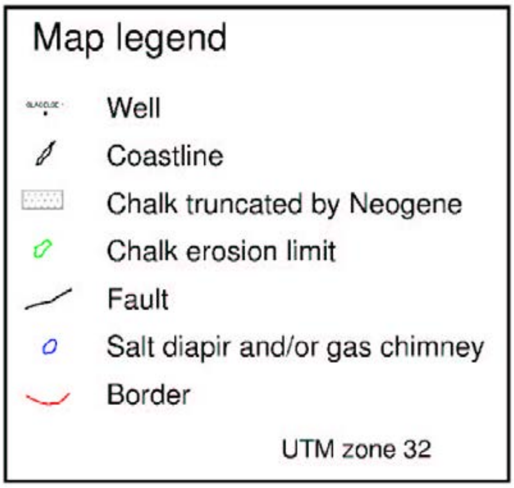

Figure 6: General map legend for maps.

3 Base Chalk map

The Base Chalk map has much the same data sources as the Top Chalk map (Baldschuhn *et al.* 2001; Britze and Japsen 1991; Britze *et al.* 1995) and a number of internal otherwise unpublished mapping projects. However, there are also additions: In the Baltic Sea northeast of the Island of Rügen an excellent base chalk map is published by Schlüter *et al.* (1997). This map is in Gauss - Krüger projection (see appendix), and in depth. The method for this depth conversion is described by Jaritz *et al.* (1991), and supported by the German Baltic sea wells G-14, K-5, H-2 and H-9 (Rempel 1992).

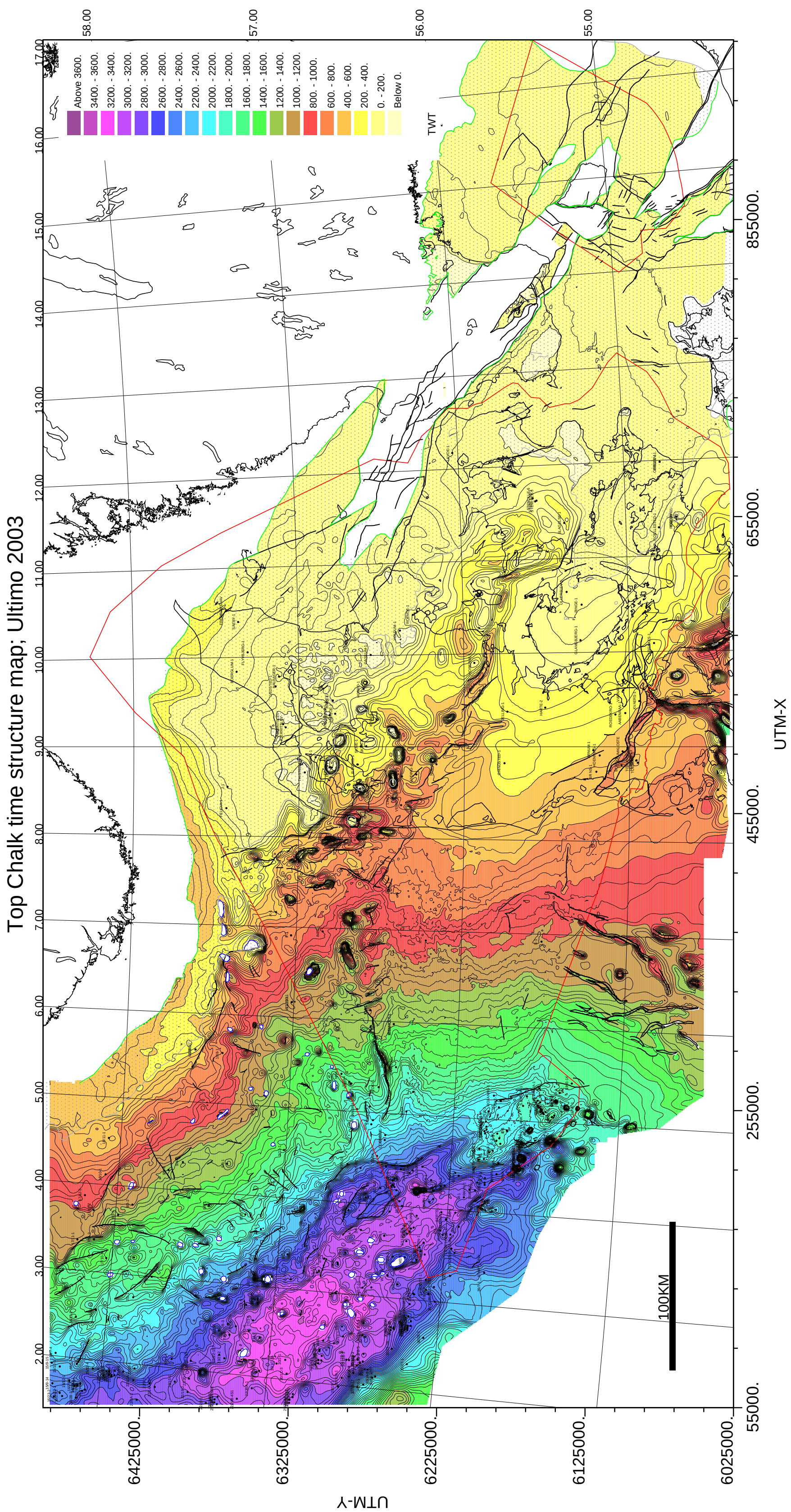

Figure 7: Top Chalk time structure map.

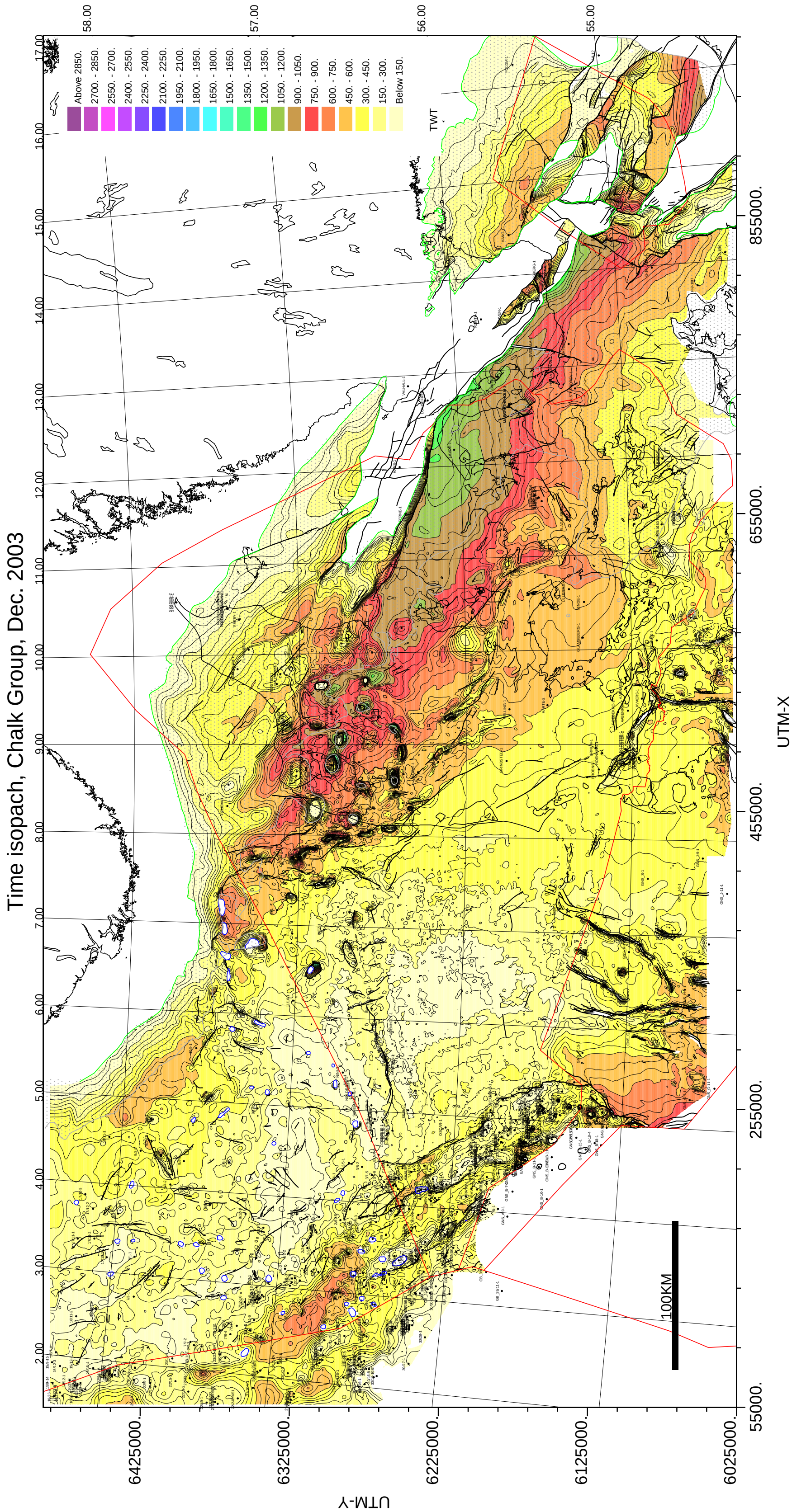

Figure 8: Chalk isopach map. Thickness in msec.

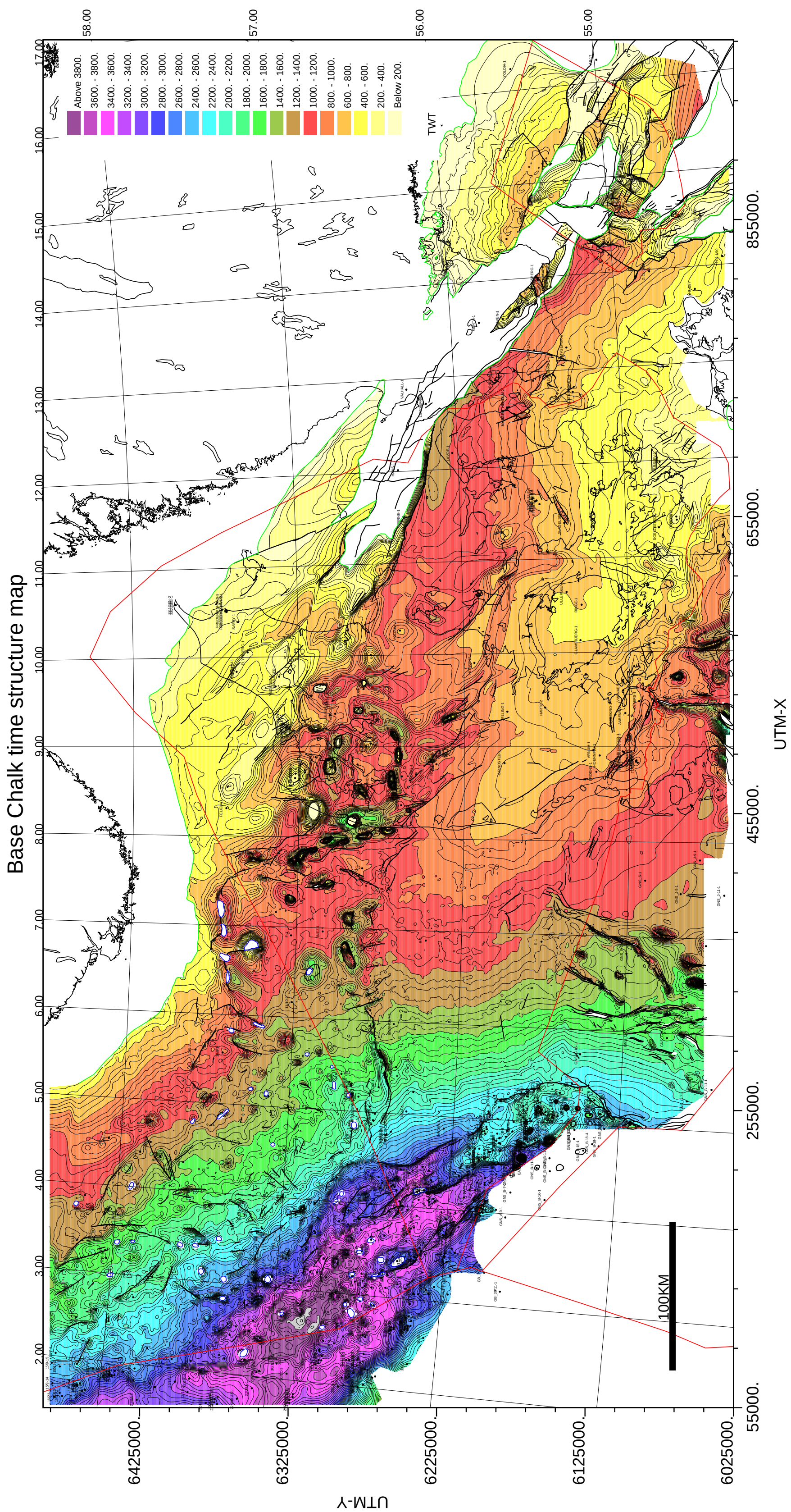

Figure 9: Base Chalk time structure map.

In the Bornholm area a compilation of various authors has been done (Kumpas 1980; Vejbæk *et al.* 1994; Vejbæk and Britze 1995; Hommel 1996). Kumpas' maps are given in the "Rikets nät" projection (see appendix) and are depth converted. Comparison to other maps (e.g. Vejbæk *et al.* 1994; Vejbæk and Britze 1995) showed discrepancies in the velocity field northeast of Chrisitiansø. As Kumpas (1980) only had the two somewhat shallow Swedish wells available (the Swedish H-1 and H-4 wells), his maps were corrected to comply with the results of the above mentioned maps. In major parts of the eastern Bornholm offshore, the Upper Cretaceous is probably resting directly on Palaeozoic strata. However, along the northeast flank of the Christiansø High thin veneers of pre-Cretaceous Mesozoic are likely to be present. Also in the Polish offshore near the coast and onshore Permian, Triassic and Jurassic strata are present northeast of the Kolobrzeg graben (e.g. Grigelis 1991).

In the Kattegat and Skagerak areas further support has been obtained from published maps (Mogensen and Jensen 1994; Vindum 2002; Jensen 1998).

4 Chalk isopach map

This map is simply produced by subtracting the top and base chalk from each other. However, in the British sector and in the Norwegian sector north of 58° N the main data source was the chalk isopach map from the Millennium Atlas (Surlyk *et al.* 2003).

A dominant feature on the isopach map is the major depocentre flanking the Sorgenfrei - Tornquist Zone to the southwest with a maximum under North Sjælland. This depocentre is proposed to be causally linked to the formation of the major inversion of the Sorgenfrei - Tornquist Zone (e.g. Gemmer *et al.* 2002; Hansen and Nielsen 2002; Vejbæk and Andersen 2002). In the same genetic category is the Hanö Bay basin, e depocentre southwest of Læsø and the Darlowo Block southeast of Bornholm. The depocentre in North Jylland also belong to this structural category where the causal inversion zone is located in Vendsyssel, but with a conspicuous overprint by salt tectonics. The depocentre flanking the Sorgenfrei - Tornquist Zone can thus be seen to continue to the northwest into the Norwegian offshore. However, there the depocentre is not abutting an inversion zone, but is instead truncated by Neogene erosion. It may therefore be surmised that the inversion zone must continue in the south - southwest Norwegian onshore, only there it vanishes due to deep Neogene erosion (e.g. Japsen *et al.* 2002).

Other lesser depocentres flanking inversion zones are found in the western German North Sea, and faintly (in this map scale) visible on the east flank of the Danish Central Graben and in the northeastern Tail End Graben (cf. Vejbæk and Andersen 2002). A depocentre in the southwestern Norwegian offshore is located over the Norwegian Central Graben and thus marks the northern termination of inversion activity (e.g. Ziegler 1995).

Areas outside the influence of inversion zones and flanking depocentres thus become rather limited. Such areas include the East North Sea Block area and the middle part of the Norwegian offshore area where thicknesses are at or below 300 msec. However, in the Norwegian area, thicknesses are also affected by Palaeogene erosion from turbidity currents such as the prominent Siri Valley (e.g. Rasmussen *et al.* in press). In the Danish area salt tectonics and high frequency (”wormy”) undulations affect thickness distribution. The ”wormy” appearance of the isopach on the East North Sea Block originates from the Top Chalk map and is supported by high data coverage and is not due to misties. The most plausible interpretation is that they represent pock marks (e.g. Clausen and Huuse 1999).

5 Depth conversion

Depth conversion of the maps is done by application of a multilayer velocity model. The method requires that a certain minimum number of wells with well-velocity surveys are available.

The multilayer velocity depth conversion method is outlined Japsen (1993, 1994). Each layer is assigned a surface velocity (V_0) and a depth gradient (K) according to the equation: $V(z) = V_0 + Kz$, where $V(z)$ is instantaneous velocity for the layer at depth z. To ensure fit to wells, lateral deviations from the average interval velocity functions are allowed through the application of the dV parameter, which is added to the V_0 parameter. The equation thus becomes:

$$V(z) = (V_0 + dV) + Kz \quad (1)$$

where dV varies laterally. Units for all parameters are given in Table 1. Detailed development of this relationship may be obtained from Japsen (1993, 1994) and only main points are given below together with some further developments.

The V_0's and K's necessary for the depth conversion can be approximated by application of simple linear regression (e.g. in a spread sheet) to cross-plots of interval velocity versus mean depth for the various sediment packages that are defined by the interpreted seismic reflectors. This fitting method is only approximate as scatter in the cross plot is not related to the dV parameter in a simple way. In this report velocity parameters are derived from detailed studies of regional velocity variations (e.g. Japsen 1998; 1999; 2000).

The computerized depth conversion of time structure maps requires that the dV parameter is given as digitally mapped velocity anomalies. Variations in dV-values may express lateral variations in lithology of a given interval or disequilibrium compaction. A positive velocity anomaly may indicate late uplift of an interval and a negative value may indicate under-compaction (overpressuring) assuming uniform lithologies in a larger area. Laterally interpolated velocity anomaly maps should be made smooth to ensure smooth interval velocities, and thus smooth depth converted maps.

The generation of maps of the velocity deviation (from the average velocity functions; the dV parameter) requires lists of these deviations together with coordinates for each well, which then can be interpolated into maps.

The dV value can be approximated from:

$$dV = \frac{(Z_b - Z_t) \cdot 2}{T_b - T_t} - (V_0 + K\frac{Z_t + Z_b}{2})$$

which uses comparison of observed interval velocity and assumed interval velocity. Here all Z's and T's are from well velocity analysis. This equation is implicitly assumed when performing linear regression on observations of interval velocity versus mean depth. This expression is, however, not exact when $K \neq 0$ and gives rise to small errors by generally producing too small dV values for $K > 0$ (most common case) and vice-versa. A more precise expression is given by:

$$dV = \frac{\Delta Z \cdot K}{\exp^{K \cdot \Delta T} - 1} - V_0 - Z_t \cdot K$$

The dV can be converted to the burial anomaly by:

$$\delta Z_b = -\frac{dV}{K}$$

The $-$ sign causes too low velocities to give rise to positive burial anomalies.

Special cases occur where positive δZ_b values can be ascribed entirely to disequilibrium compaction caused by excess pore fluid pressure. This occurs mainly in the Palaeogene and Chalk successions in the Central graben area. An approximate estimate on the amount of excess pressure ΔP is given by:

$$\Delta P = \delta Z_b \cdot (\rho_r - \rho_{br}) \cdot G$$

where ρ_r and $\rho_b r$ are densities of rock and brine and G is the gravity constant. Assuming $\rho_r = 2000 kg/m^3$ and $\rho_{br} = 1000 kg/m^3$ then 100m of burial anomaly is roughly equivalent to 1 MPa. Pressure estimated from velocity may deviate by as much as 15% compared to observed pressure, but has the advantage of fast pressure mapping and much larger data coverage because velocity data are much more abundantly available than reliable pressure data.

Depth conversion using the linearly increasing instantaneous velocity assumption ($V_i = V_0 + Kz$) is done layer by layer downwards. The thickness of a layer is found from:

$$\Delta Z = \frac{1}{K}(V_0 + dV + (K \cdot Z_t))(\exp^{K\Delta T} - 1) \qquad (2)$$

where ΔT is one-way time. In the case of no velocity increase with depth ($K = 0$) the equation simplifies to:

$$\Delta Z = (V_0 + dV) \cdot \Delta T \qquad (3)$$

To back calculate depth thickness to time thickness:

$$\Delta T = \frac{1}{K} \cdot Log \left[1 + \Delta Z \cdot \frac{K}{V_a} \right] \qquad (4)$$

where V_a is instantanous velocity at the top of the interval:

$$V_a = V_0 + dV + K \cdot Z_t$$

Direct calculation of interval velocity may be done from:

$$V_{int} = \frac{2}{\Delta T}[V_0 + dV + K \cdot Z_t](e^{K\Delta T/2} - 1)$$

where V_{int} is the interval velocity of the mapped package.

In some cases it may be convenient to reconstruct dV information from old maps. This can be for the purpose of re-using and extend the velocity anomaly map, or to use the mapped velocities with new functions. This may be done according to

$$V_0 + dV = (V_{int} - K \cdot Z_t)/(1 + K \cdot \Delta T/4)$$

The interval velocity (V_{int}) must therefore be available, for instance by subdividing meter thickness maps with time thickness maps. It is noted that only prior information on the velocity gradient (K) must be known. The expression is only approximate, but may suffice for most purposes.

Symbol	**Meaning**	**Unit**
ΔZ	Thickness	*meters*
V_0	Surface velocity	$m/sec.$
dV	Velocity deviation	$m/sec.$
K	Velocity gradient	$sec.^{-1}$
Z_t	Depth to top of layer	*meter*
Z_b	Depth to base of layer	*meter*
T_t	Two-way time to top of layer	*sec.*
T_b	Two-way time to base of layer	*sec.*
ΔT	Thickness in one-way reflection time	*sec.*

Table 1: The symbols in depth conversion and their units.

5.1 Post-chalk interval

The Cenozoic velocity model consists of a single layer onshore Denmark and farther east, and two layers west of the Danish mainland (Table 2). The two layers are divided at a mid Miocene reflector approximately corresponding to the top of the overpressured section (Upper and Lower Post Chalk Group in Table 2). We use parameters for these layers as determined by Britze et al. (1995) and Japsen (1999). The parameters are applicable to most of the North Sea as they are based on a large well data base from the entire North Sea (e.g. Japsen 2000).

The two layered model for the North Sea area is only applied, where mid Miocene reflector is interpreted (Rasmussen *et al.* in press; Fig. 10). The velocity function parameters for this area are termed "Upper Post Chalk Group" and "Lower Post Chalk Group" in Table 2. As this horizon has not been tied precisely in the wells in the area, no velocity anomaly map is applied for the interval above. For the interval below down to Top Chalk, velocity anomalies are mapped to ensure tie between the wells and the depth converted Top Chalk map. Depth values (Z_t in the equations in previous section) for the top of the Lower Post Chalk Group is therefore only approximative, and all uncertainty in the chalk overburden velocity field is ascribed to the Lower Post Chalk Group. This is assumed to be a reasonable approach, as earlier studies suggest the main cause for velocity variation to be attributed to overpressuring, which occurs below the mid Miocene reflector (e.g. Japsen 1993; 1994; 1999). This reflector therefore is often referred to as "Near Top Overpressure".

The velocity mapping in the Norwegian sector only applies a one layer model down to the Top Chalk and originates from an internal unpublished mapping campaign. In order to get a continuous velocity field, a smooth merge of this velocity field with the average velocity field from the two layer model down to Top Chalk for the Danish sector has been performed.

Interval	V_0	K
Upper Post Chalk Group	1725	0.4
Lower Post Chalk Group	1517.2	0.6
Onshore functions	1650	0.62
German North Sea	1725	0.5

Table 2: Velocity parameters for depth conversion down to the Top Chalk (Britze *et al.* 1995; Japsen *et al.* 1999).

North of 58° and in the British sector published depth maps have been available (Surlyk *et al.* 2003). In order to incorporate these maps also in the reflection time domain, the Norwegian sector velocity field has been inverted to surface velocity (as described in the previous section), extended into the British sector and used inversely on the depth maps (equation 4 in previous section). The velocity parameters for this operation are equal to "Upper Post Chalk Group" in Table 2.

No well velocity data have been available for the German sector, and the published maps are all in depth (Baldschuhn *et al.* 2001). Therefore an inversion of the mapped velocity field for the south part of the Danish area to a surface velocity field has been performed using parameters termed "German North Sea" in Table 2. These surface velocities have been extended to cover the entire german sector to allow inversion of the depth map to time. Due to lack of well control, the depth map must be considered more precise than the time map.

The Danish onshore areas are depth converted using parameters termed "Onshore function" in Table 2. A major part of this area has been depth converted previously (Britze and Japsen 1991), but this work has been inverted back to surface velocity as described in the previous section, as no dV - maps were avalable from that study. This has allowed an extension of the velocity field to cover areas not previously published. In large areas of the Danish onshore and western Baltic, the top Chalk is equivalent to the base Quaternary (Figs. 4, 5). The primary data source is here water wells and shallow seismic maps already given in meters. Due to expected large uncertainties in velocity of the Quaternary and other overburden on the Chalk (sometimes water), velocity mapping has been considered futile, and a universal velocity of $2km/sec$ has been assumed in these areas to make depth and time maps equal.

The time map as well as the depth map have been corrected for the remaining misties to wells by interpolating these errors and adding them to the maps. In this way also wells without velocity survey can help in refining depth conversion. Following this operation, the mean error on the time and depth maps at well sites is reduced to 0.22 msec and 28 cm with a standart deviation of 11 msec and 12 m approximately at well sites. Much of this deviation is inevitable due to the large grid spacing of 500 m.

As has also been shown by Japsen (1998; 2000) the parameters are sufficiently well determined to allow rough estimation of excess fluid pressure in the Lower Post Chalk Group. The pressure map in Fig. 12 shows the well-known southeastward decrease in excess fluid pressure from the maximum in the southwestern Norwegian offshore (e.g. Megson and Hardman 2001). In addition, however, a drop towards the northeast away from the Central Graben is also visible. This northeasterly pressure drop is faster along the Norwegian - Danish borderline, where Paleocene sands are known to occur (e.g. Rasmussen *et al.* in press), thus suggesting partial pressure drainage through these sands. Sand injection and other sand mobilisation phenomena are thus likely to occur along the Siri Trend northeast of the Central Graben. The change from southeasterly decreasing fluid pressure in the axial part of the Central Graben to easterly decreasing pressure along the northeastern margin of the Central Graben are also mimicked by Chalk Group water zone pressure as the Lower Palaeogene and the Chalk generally are in pressure communication (e.g. Moss *et al.* 2003). This may be of major importance for the prospectivity of the under-explored chalk along Northeastern margin of the Danish Central Graben as fluid contacts in chalk reservoirs almost invariably are affected by dynamic water zones (e.g. Thomasen and Jacobsen 1994; Vejbæk *et al.* in press).

5.2 Chalk interval

In the case of Chalk, Japsen (2000) has erected a 4 layer composite model for standard velocity depth trends:

Interval	V_0	K	V_b
$0 - 900m$	1550	1.3	2720
$900 - 1471m$	920	2	3862
$1471 - 2250m$	1950	1.3	4875
$> 2250m$	2625	1.0	-

Table 3: Velocity parameters for depth conversion from Top Chalk to base Chalk (Japsen 2000). V_b is instantaneous velocity at segment interface.

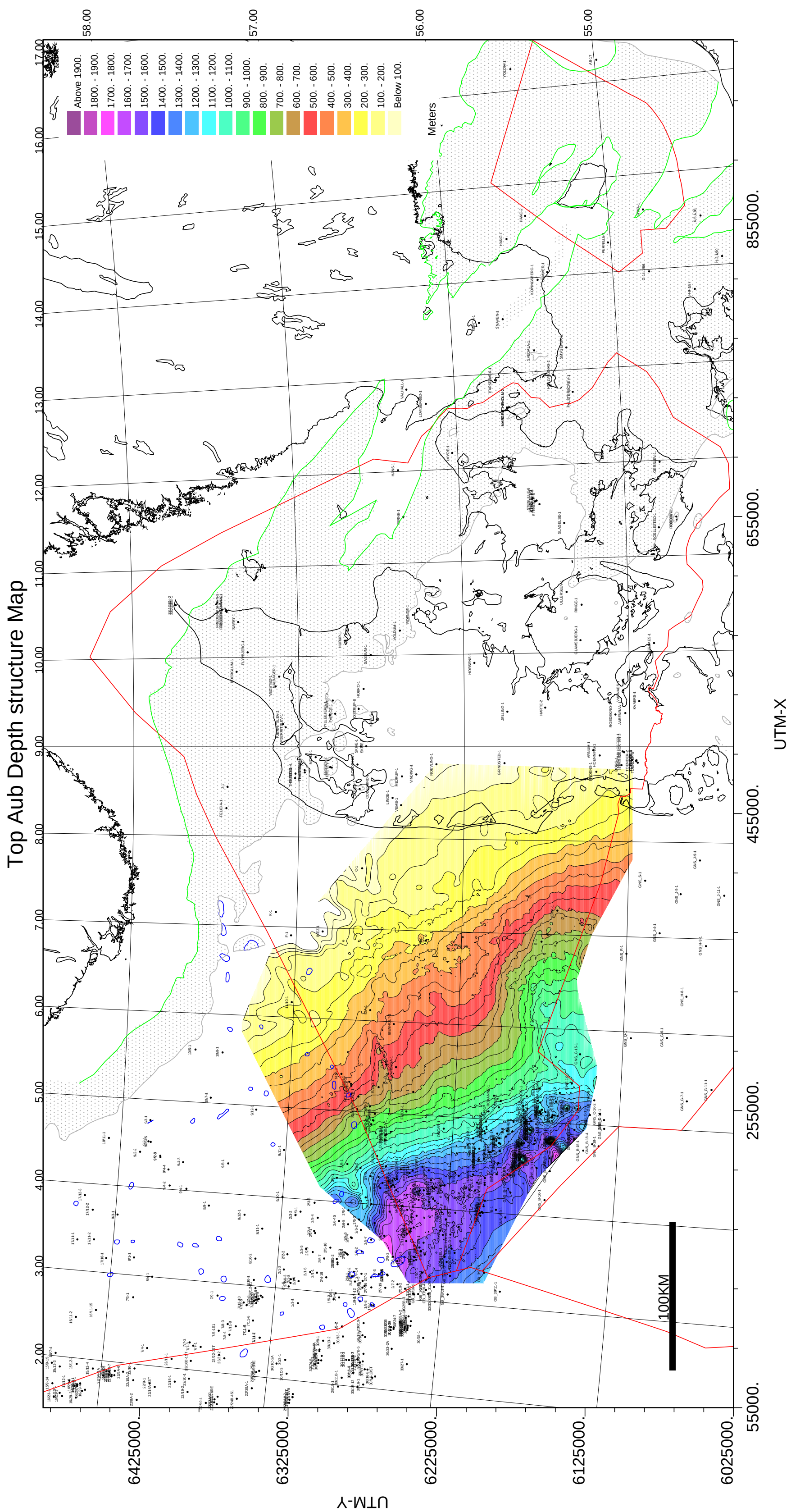

Figure 10: Mid Miocene depth structure map. dV values for Top Chalk depth conversion are assigned entirely to below this horizon (mod. from Rasmussen *et al.* in press). C.i.= 50m.

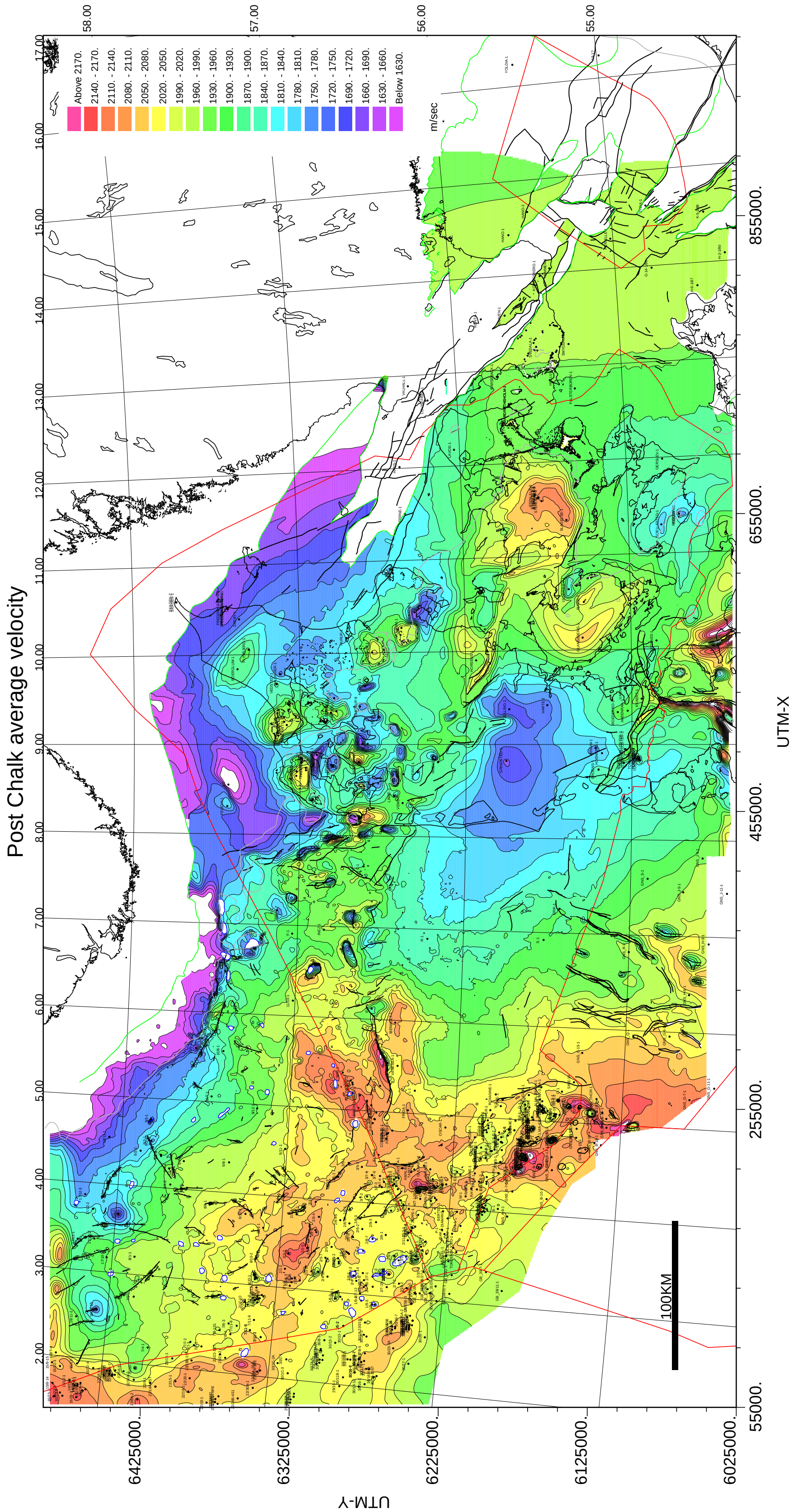

Figure 11: Post Chalk Group average interval velocity. This velocity map is the direct relation between Top Chalk time and depth maps. C.i.= 30m/sec.

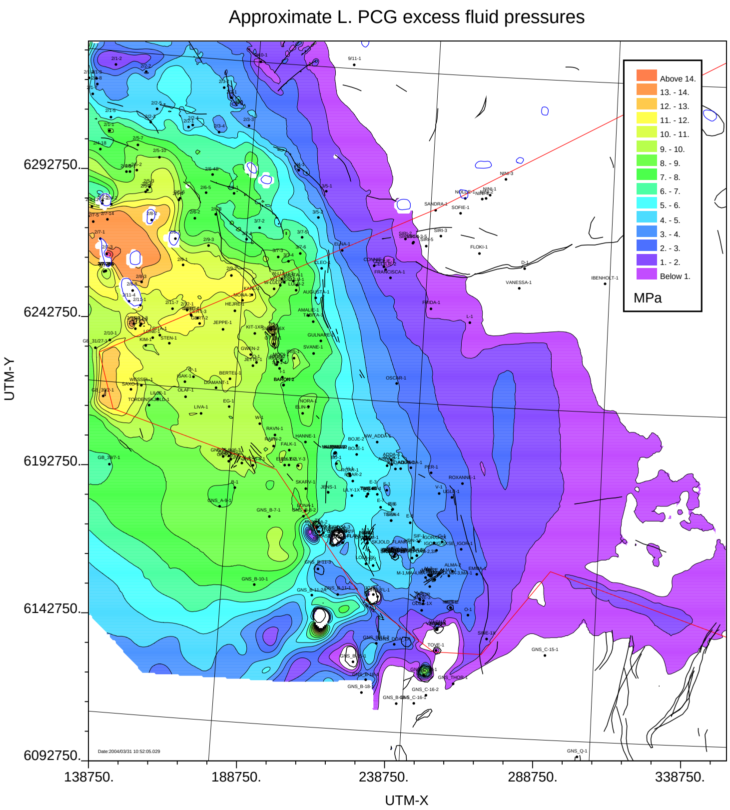

Figure 12: Over pressure for the Lower Post Chalk Group as calculated from velocities. The Siri Valley sand system is clearly dissipating pressure locally. C.i.= 1MPa.

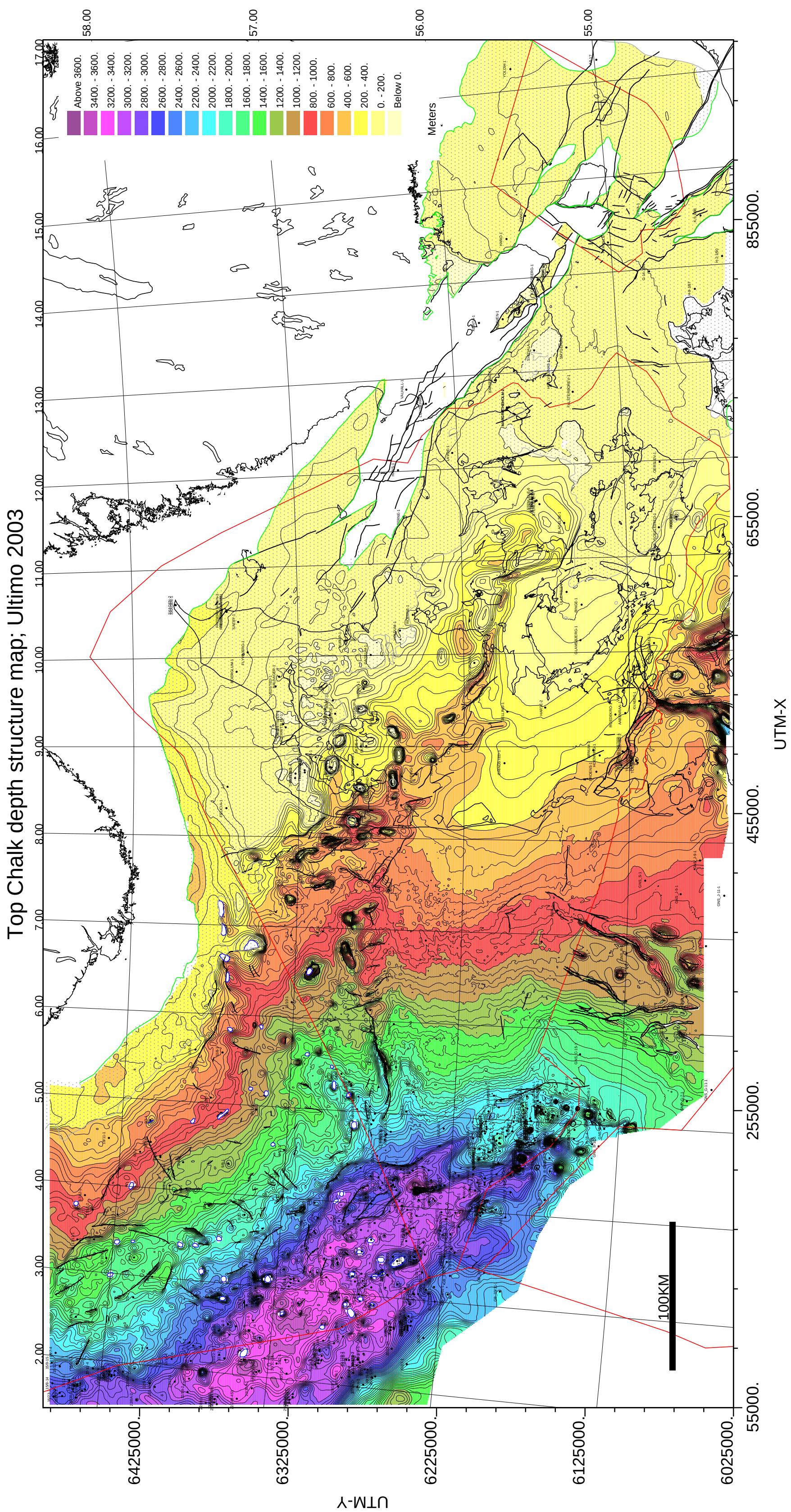

Figure 13: Top Chalk Depth structure map. See also enclosure 1. C.i.= 50m.

In this case depth conversion is done by:

$$\Delta Z = \sum_{1}^{n} \frac{1}{K_n}(V_{0n} + dV + (K_n \cdot Z'_t))(\exp^{K_n \Delta T'} - 1) \tag{5}$$

where n refer to the n'th segment in a chalk succession of the above model and Z'_t is the top of the n'th layer, where tops internally in the unit are given in Table 3 (Fig. 14). $\Delta T'$ is in this case referring to the time thickness of each segment of the model in a given succession. In practice the above equation is only applied to find out what segments are present in the depth interval of interest, and for the lowermost depth segment that has an abitrary depth to base. When the segments are determined equation 4 is applied to subtract $\Delta T'$ from ΔT in the downward depth conversion process.

A problem in composite velocity models is the determination of dV for thick sections that contain several velocity model segments. This is done by first depth converting with $dV = 0$ and calculating dV approximately according to:

$$dV = \frac{(Z_b - Z_t) \cdot 2}{T_b - T_t} - \frac{(Z_b - Z_t)}{\Delta T}$$

where ΔT is the erroneous time thickness based on equation 5 assuming $dV = 0$ and the Z's and T's are well data (hard data). This gives an approximate velocity anomaly. If better resolution is needed, iteration is the only option by applying equation 5. Convergence may be obtained by updating dV according to:

$$dV = dV' + dV' \cdot \frac{T_{err}}{T_b - T_t} \text{ for } dV > 0$$

and

$$dV = dV' - dV' \cdot \frac{T_{err}}{T_b - T_t} \text{ for } dV < 0$$

where $T_{err} = 2\Delta T - (T_b - T_t)$. A suitable convergence criteria may be $|T_{err}| < 0.0002$ or one fifth of a millisecond. As opposed to the first estimate on dV, the iteratively determined dV is much more precise (as given by T_{err}.

In the multisegment velocity model, determination of the burial anomaly is also more complex. First the mean normal velocity (V_n) for the interval of interest is found from:

$$V_n = \frac{\Delta Z}{\Delta T} - dV$$

The mean reference depth (Z_m) can then be found from:

$$Z_m = \frac{V_n - V_0}{K}$$

where the relevant V_0 and K are determined by comparison between V_n and the instantaneous velocity at the base of each segment (V_b) as given in Table 2. It is noted that Z_m is only approximately equal to the mean depth of the interval. Knowing Z_m, the burial anomaly can be calculated from:

$$\delta Z_b = \frac{\frac{\Delta Z}{\Delta T} - V_0}{K} - Z_m$$

In this case the relevant V_0 and K are determined by comparison between $\frac{\Delta Z}{\Delta T}$ and the velocity at the base of each segment (V_b). This means that the velocity constants may be different for the determination of Z_m and δZ_b (Fig. 14).

The resulting interval velocity shown in Fig 15 clearly shows that primary control on velocity variation is depth of burial. By studying the dV map instead, an illustration of effects other than depth of burial such as overpressuring, exhumation and lithology may be obtained (Fig, 16). It is clear that velocity in the Central Graben is below the normal trend, and that velocities are above normal near the Norwegian coast and most of the Danish mainland with an increasing tendency to the northeast. If anomalies on the dV map can be referred to only to exhumation and overpressuring, the burial anomaly map may provide estimates on how much exhumation has occurred or how large the overpressure is (Fig. 17; Japsen 2000). The interpreted overpressure (burial anomaly divided by 100 gives pressure in MPa as discussed previously) in the Central Graben is roughly similar in shape and magnitude to the one for the Palaeogene (Fig. 12) which is consistent with the observation that excess pressure in the Lower Palaeogene and the Chalk generally are the same (e.g. Moss *et al.* 2003). Details are, however, somewhat different on a local scale which may be partly due to a reduced data control, as fewer wells penetrate the chalk. Local positive anomalies are seen around some salt structure suggesting local pressure dissipation through faults associated with the salt movements. Positive burial anomalies are characteristic for the areas close to Norway and most of the Danish onshore. It has been interpreted to reflect Late Cenozoic uplift and is consistent with estimates by other means (Japsen and Bidstrup 1999; Japsen 2000). Interpretation of the burial anomaly in Scania and the Bornholm region should be done with caution, as the Upper Cretaceous there contain lithologies other than Chalk (e.g. Kumpas 1980; Sivhed *et al.* 1999; Erlström 1990; 1994). In these areas some support has been gained from seismic stacking velocities corrected for velocity heterogeneity (e.g. Al-Chalabi 1981; Vejbæk and Britze 1994).

Time maps as well as depth maps have been corrected for the remaining misties to wells by interpolating these errors and adding them to the maps. In this way also wells without velocity survey can help in refining depth conversion. The mean error following this operation is difficult to estimate because some wells were deliberately held out of this process due to local structural complexity. Also a number of wells were ending somewhere in the middle of the chalk. They may contribute to the mapping of the chalk velocity field, but not as control on depth conversion to base chalk. Mean error at well sites on the time and depth maps is, however, estimated to be 1 msec and 1 m with a standart deviation of 10 msec and 11 m approximately. Again much of this uncertainty is attributed to the grid density of 500 m.

6 Discussion

Chalk deposition took place on a background of regional subsidence following the former mainly Late Jurassic rifting that strongly abated during the Early Cretaceous. The Chalk Group isopach map of the North Sea region (Fig. 18, enclosure 3) suggests local deviations from the background regional subsidence. Anomalously thin or even absent Chalk Group deposits are for instance recorded in the Danish Central Graben, the West Netherlands Basin, the Sole Pit Basin and the Sorgenfrei Tornquist Zone (see Fig. 20 for location). Zones of anomalously thick Chalk Group deposits flank these thinned areas. This is particularly evident along the Southwest margin of the Sorgenfrei Tornquist Zone. These anomalies are suggested to be caused mainly by inversion movements during Late Cretaceous - Palaeogene times (e.g. Mogensen and Jensen 1994; Vejbæk and Andersen 2002). The causal link between the inversion zones and their flanking depocentres has been investigated quantitatively by Gemmer *et al.* (2002) and Hansen and Nielsen (2002; 2003).

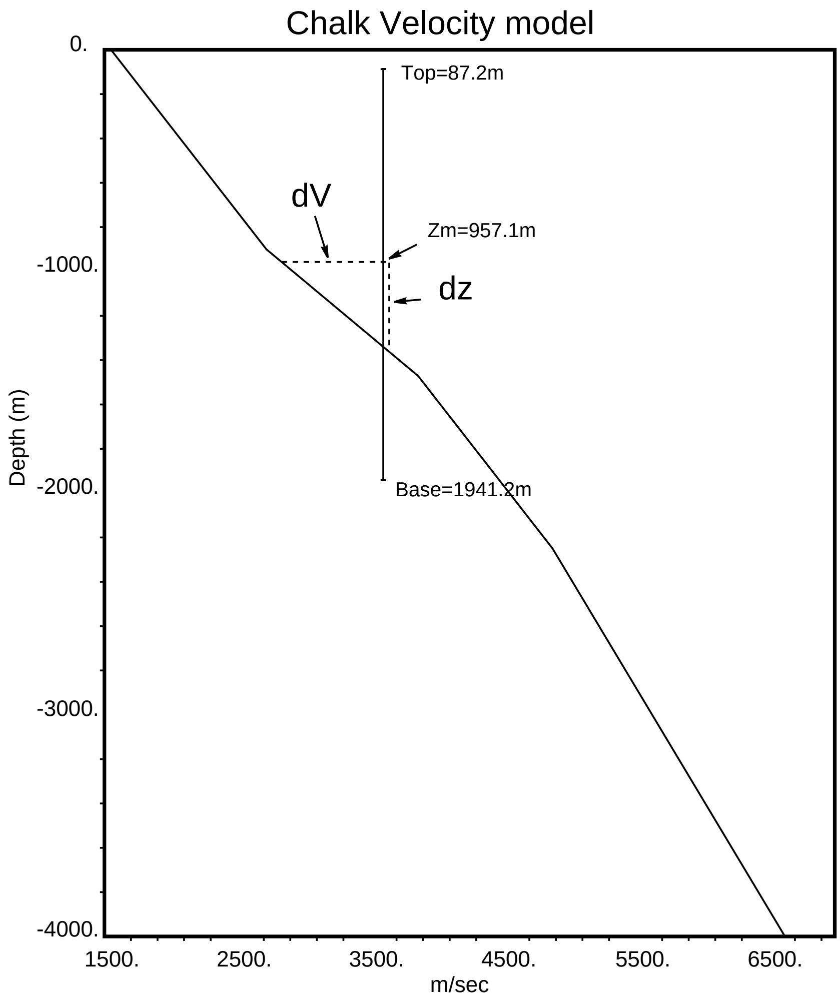

Figure 14: Chalk velocity model. A sample location is shown to illustrate the concept of burial anomaly (δZ_b) and velocity anomaly (dV). Note that these two quantities may refer to different segments of the model. Note that Z_m is not exact midpoint depth; see text.

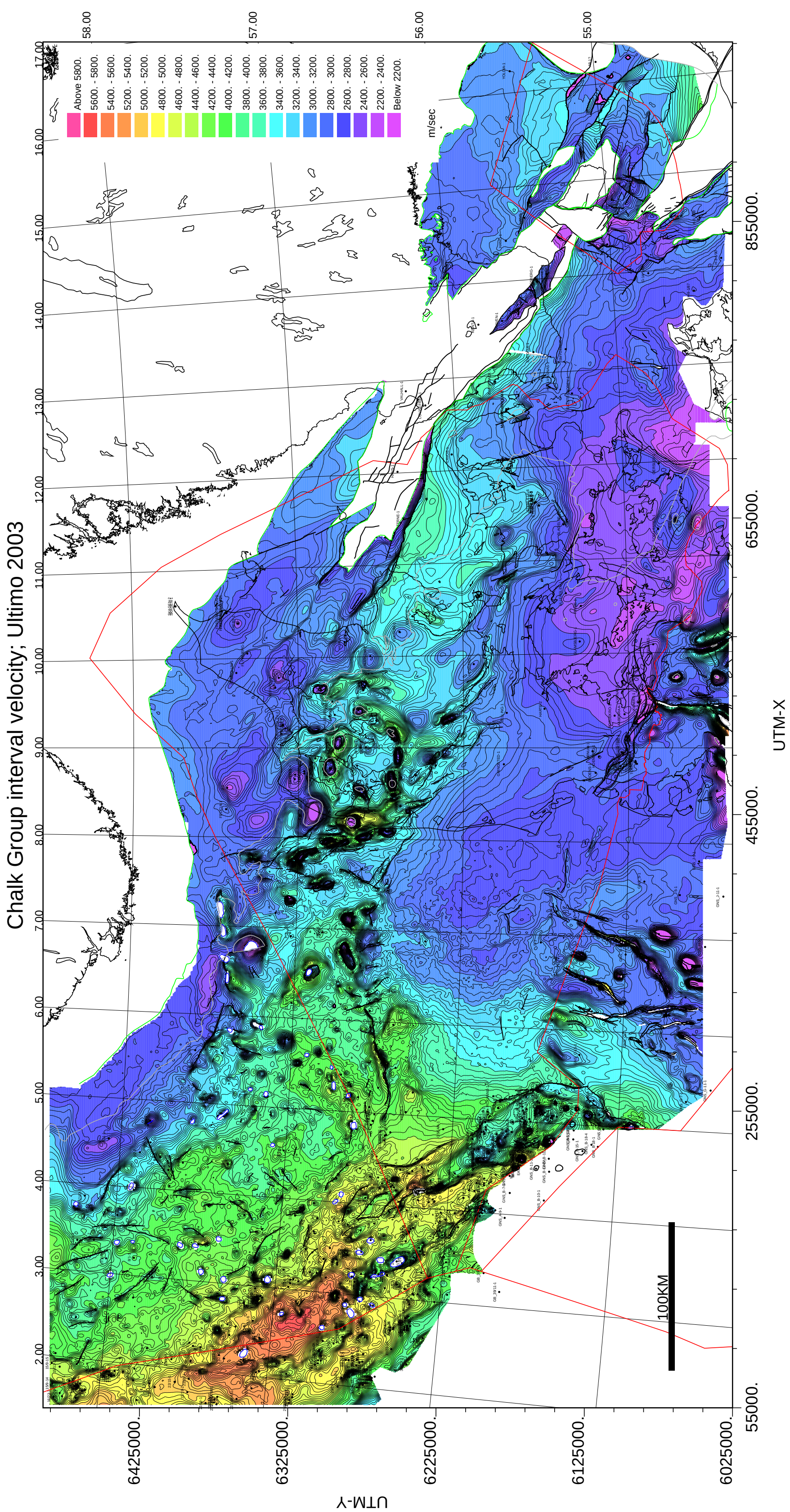

Figure 15: Chalk Group average interval velocity. C.i.= 50m/sec.

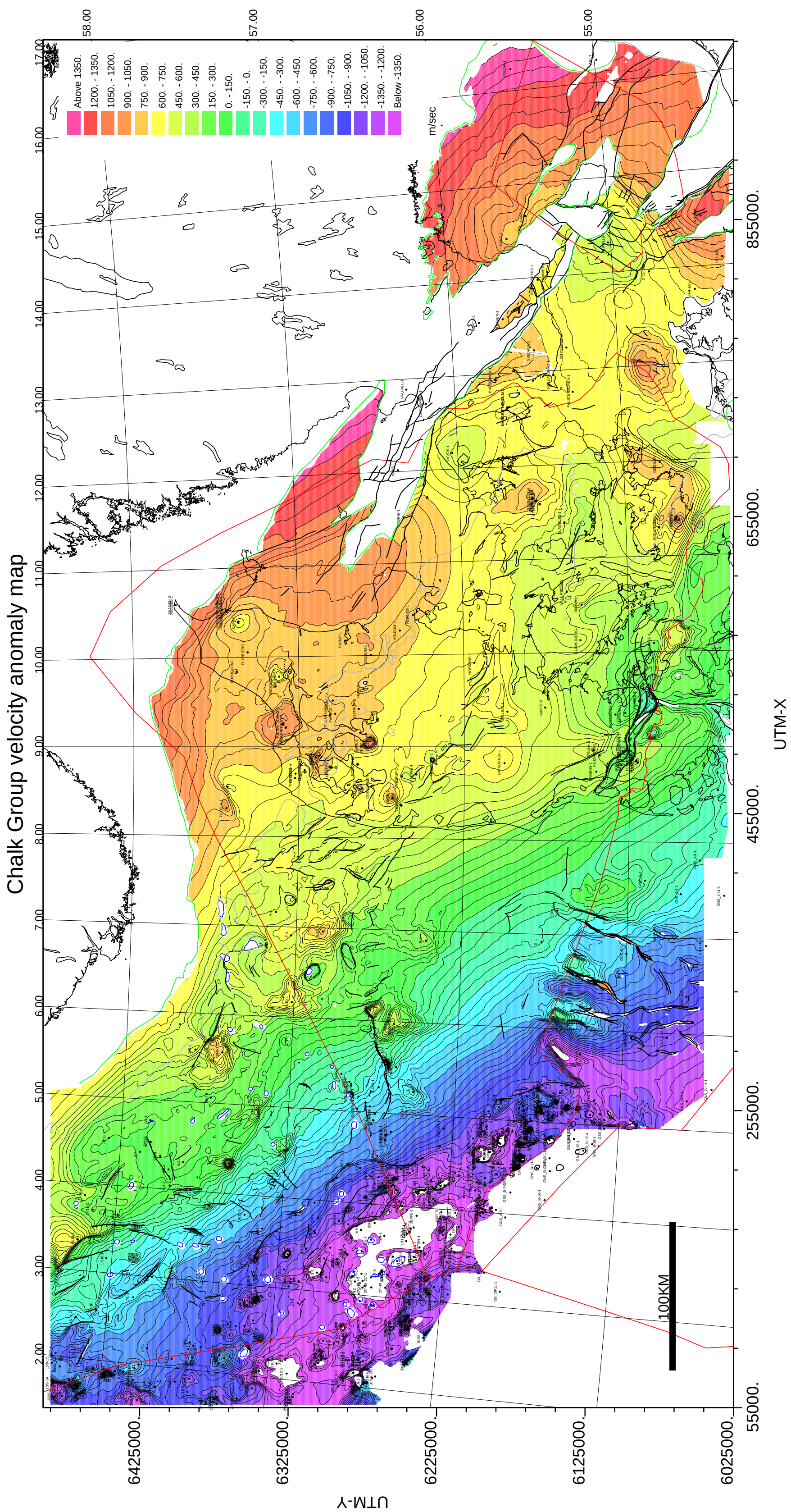

Figure 16: Chalk Group velocity anomaly map. C.i.= 50m/sec.

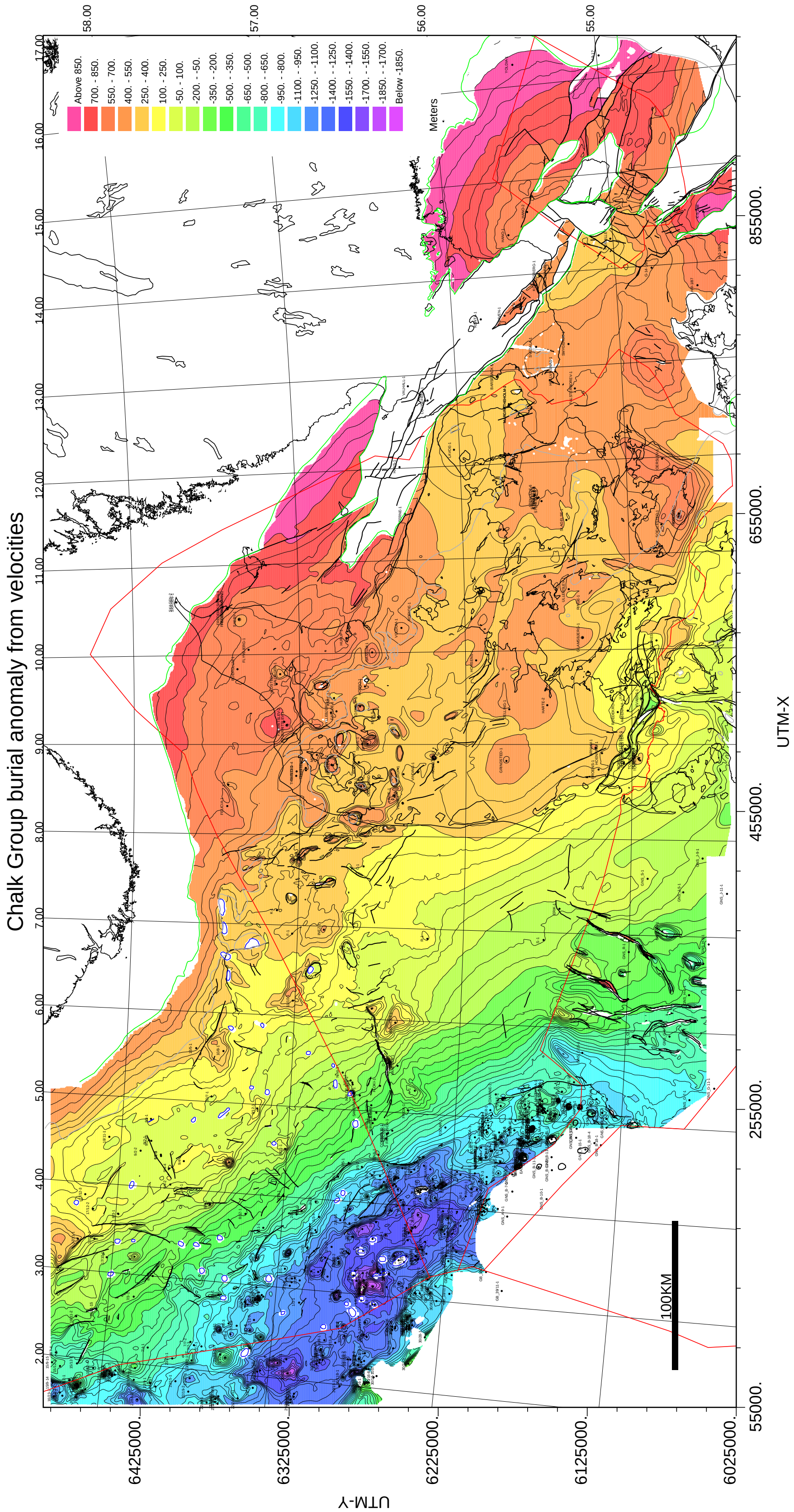

Figure 17: Chalk Group burial anomaly map. Anomalies are derived from velocity analysis. C.i.= 50m.

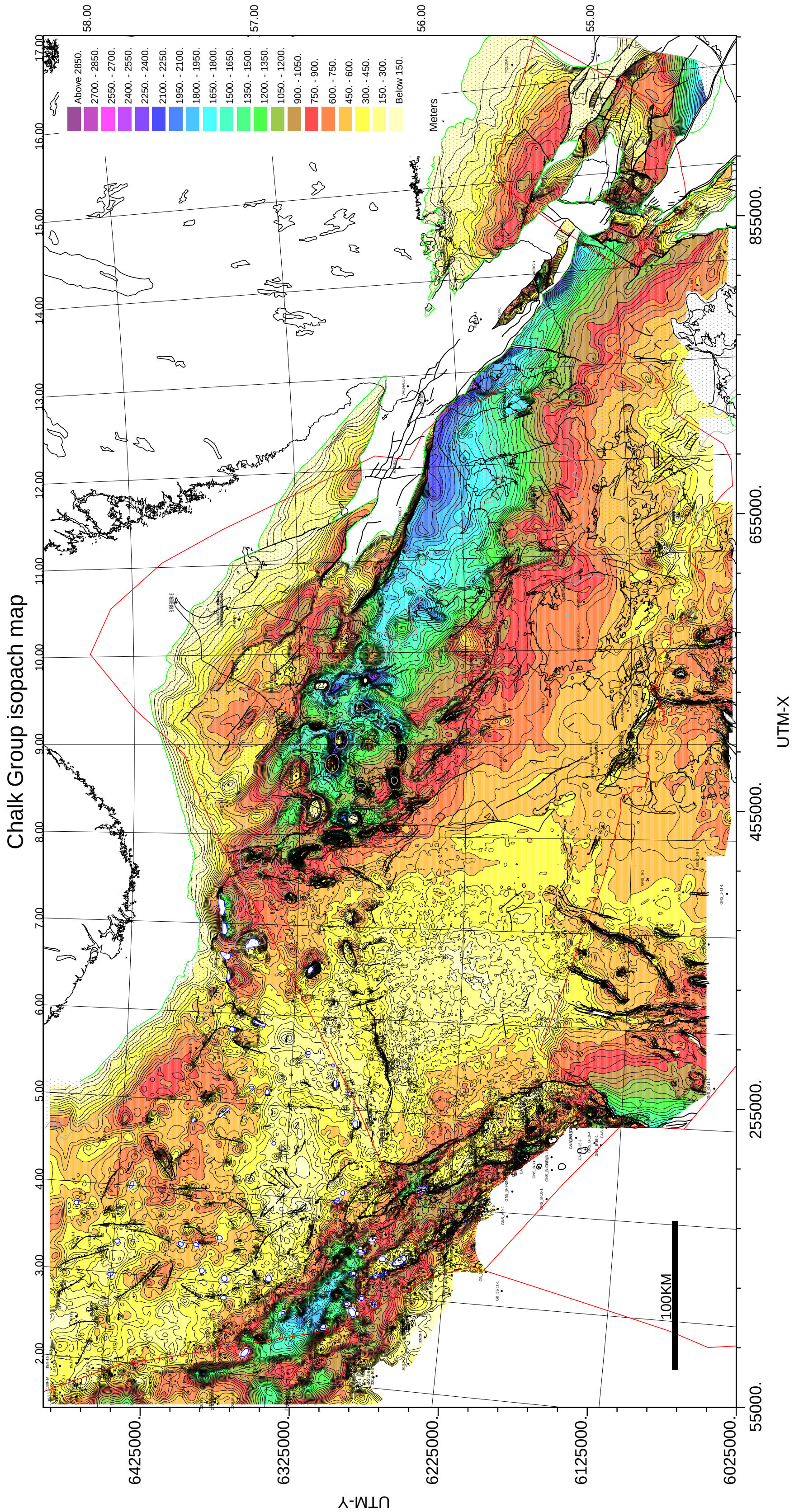

Figure 18: Chalk isopach map. Thickness in meters. See also enclosure 3. C.i.= 50m.

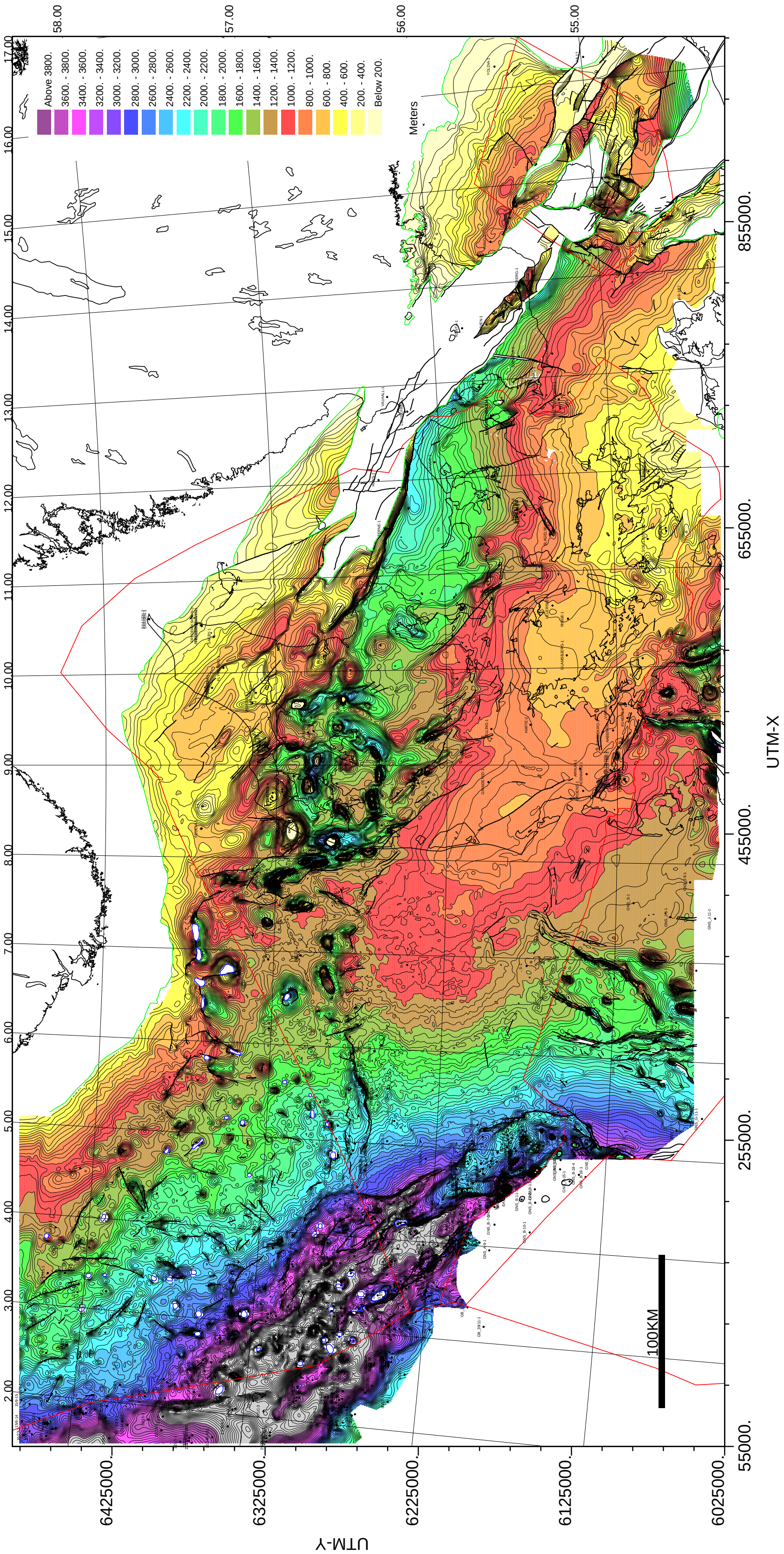

Figure 19: Base Chalk depth structure map. See also enclosure 2. C.i.= 50m.

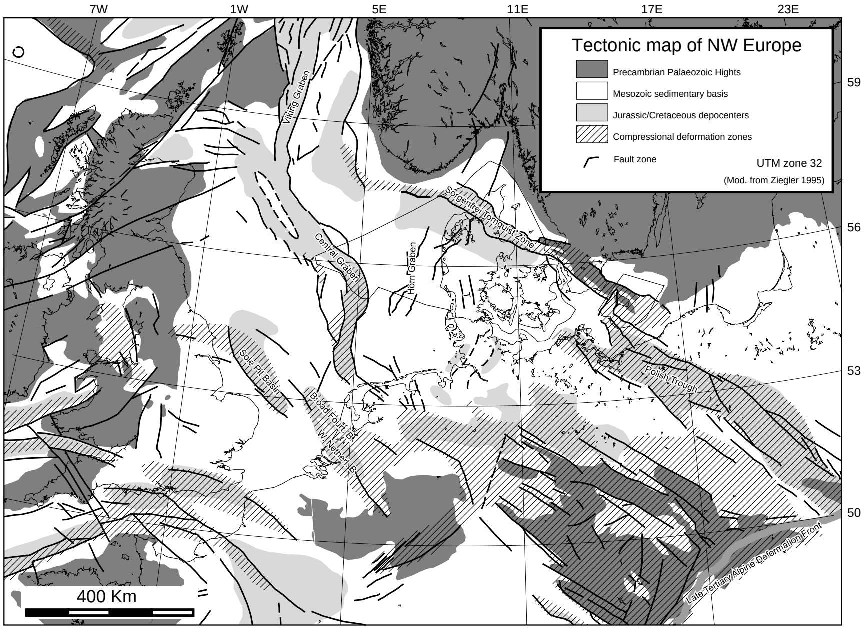

Figure 20: Northwest European zones of Cretaceous - Palaeogene inversion tectonism (mod. from Ziegler 1995).

Structural inversion of sedimentary basins is the process by which former areas of subsidence and sedimentation formed in an extensional stress regime are uplifted under the influence of compressive stress. The location of these former depocentres may be evident from Fig. 21. The inverted areas are closely associated with moderate to strongly fault controlled mid-Mesozoic subsidence preceeding Late Cretaceous inversion with the exception of the Höllvik Graben, the Egersund Basin and the Søgne Basin. These thus include the Sorgenfrei - Tornquist Zone (e.g. Mogensen and Jensen 1994; Mogensen 1995) and the Central Graben (e.g. Vejbæk and Andersen 2002).

Inverted zones also include the red zones in Fig. 21 denoting areas of eroded pre-Cretaceous Mesozoic with the exception of the Skurup High, and the East North Sea Block. In Scania Triassic outliers at the northeast limit of the Sorgenfrei - Tornquist Zone suggest that at least some of these areas may have formed pre-Cretaceous Mesozoic depocentres such that the present lack of these sediments may be due to erosion caused partly by inversion (Erlström *et al.* 2001).

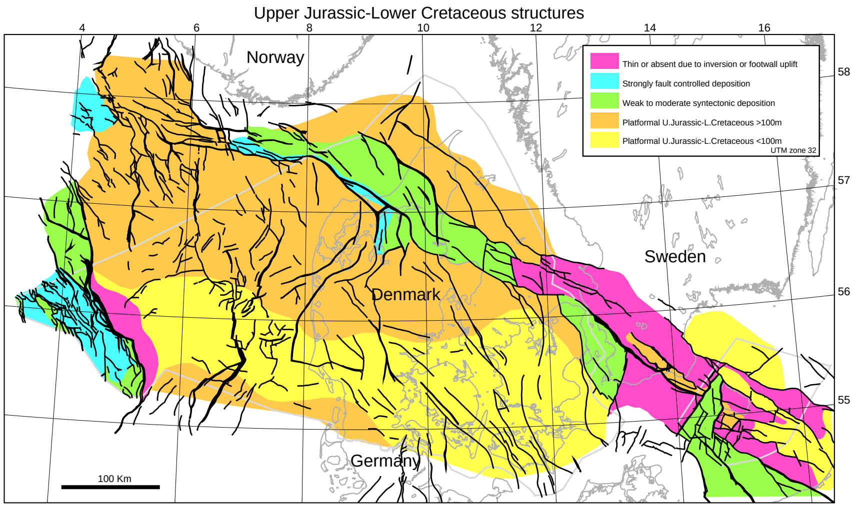

Figure 21: Upper Jurassic - Lower Cretaceous basin framework. tectonism (Vejbæk 1997).

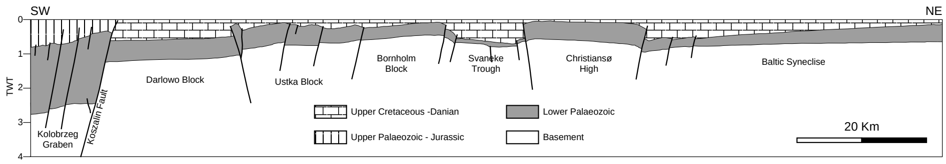

Figure 22: Profile from the southeast Bornholm offshore. The area between the Kolobrzeg Graben and the Christiansø High (both included) is clearly affected by inversion uplift (Vejbæk and Andersen 2002).

In the Bornholm area, the inversion zones becomes more diffuse as it includes the area between (and including) the Gryfice Graben and the Christiansø High with intermittent (and causally linked) flanking depocentres (Fig. 22). The Bornholm area constitues a dextral sidestep of the inversion zone to its continuation into the Polish Trough (e.g. Vejbæk and Andersen 2002). This area also contains notable exceptions to the rule by displaying inversion structures, where preceeding Mesozoic depocentres are rather unlikely to have existed. Here the Upper Cretaceous is resting more or less directly on Palaeozoic northeast of the Kolobrzeg Graben.

As discussed in section 4, the inversion in the Sorgenfrei - Tornquist Zone continues to the northwest south of the Børglum Fault with the main North Jylland Chalk depocentre as the causally linked flanking depocentre abutting the inversion zone. The continuation of the mid Mesozoic depocentre into the Farsund Basin may thus constitute a continuation of the inversion zone and possibly continuing even farther onshore the Norwegian mainland via the Varnæs Graben along the Eigerøy Horst. No direct evidence for the continued inversion zone is found due to deep Neogene erosion in southern Norway (Japsen *et al.* 2002), but an otherwise in-explicable northeasterly thickness increase in the Norwegian offshore may be interpreted as a flanking depocentre to an inversion zone.

The other main location of Late Cretaceous - Palaeogene inversion is the Central Graben. Here inversion movements are much subdued in comparison to the movements in the Sorgenfrei - Tornquist Zone, and inversion becomes negligible northwards in the Norwegian sector. In the Danish Central Graben inversion is confined to zones that do not include all of the former Mesozoic depocentres (Vejbæk and Andersen 1987; 2002; Fig. 23). The somewhat subdued tectonic movements makes this area better suited for studying details in the development of the inversion. It has thus been proposed that continued inversion took place, but with at least 4 distinct major pulses in the 1: Pre-Campanian - Santonian, 2: Campanian, 3: Maastrichtian and 4: Post- Danian (Andersen et al. 1990; Vejbæk and Andersen 1987; 2002). The sub-phases are characterized by a temporal change in structural style from narrow zones associated with pervasive reverse faulting along pre-existing normal faults to gentle basinwide flexuring and folding with only minor associated reverse faulting.

The chalk in the Central Graben area is an important carrier of oil and gas by supplying 80% of Danish oil production and also a major contributor of oil and gas production in Norway and the Netherlands (Fig. 27). The traps range from inversion generated anticlines (e.g. Valhall, Roar, Tyra, South Arne) over salt domes with some degree of inversion overprint (e.g. Dan, Ekofisk, Svend) to salt diapirs (e.g. Skjold, Harald). Also stratigraphic traps may play a major role (e.g. Halfdan, Adda). The presence of these traps owe their existence to some combination of over-pressuring and early hydrocarbon invasion for preserving reservoir quality despite the large burial depths (e.g. Anderson 1999). Also the position right above the main Upper Jurassic source rock seems to be a necessary condition (e.g. Anderson 1999, Surlyk et al. 2002). This is caused by the generally very low permeability which precludes long distance migration, and even keep accumulations in hydrodynamic disequilibrium (e.g. Dennis *et al.* 1998; Vejbæk *et al.* in press).

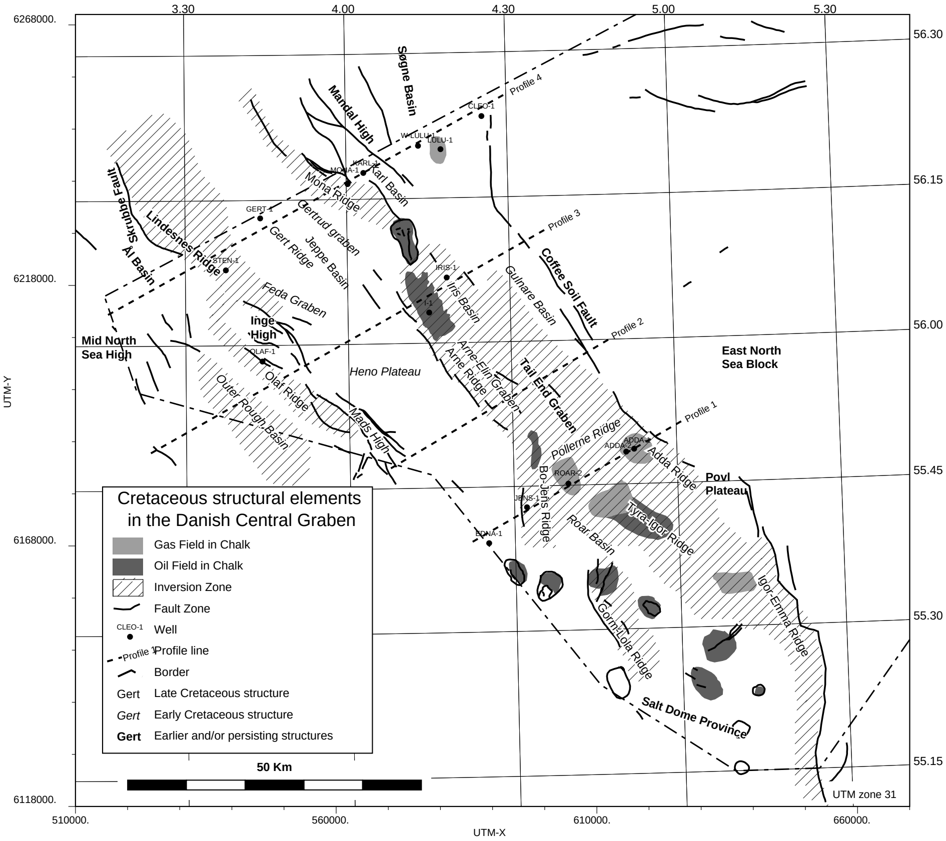

Figure 23: Main inversion zones in the Danish Central Graben (from Vejbæk and Andersen 2002).

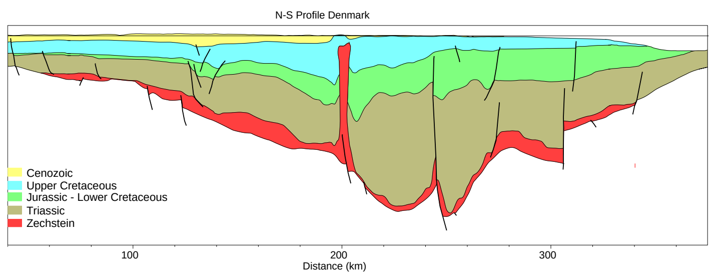

Figure 24: North - south depth profile across the Ringkøbing - Fyn High. The Chalk Group is shown in light blue (see Fig. 26 for location).

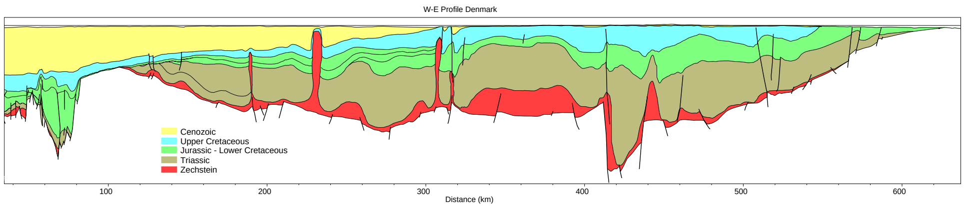

Figure 25: West - east depth profile across the Danish Central Graben and along the central parts of the Norwegian - Danish Basin (see Fig. 26 for location).

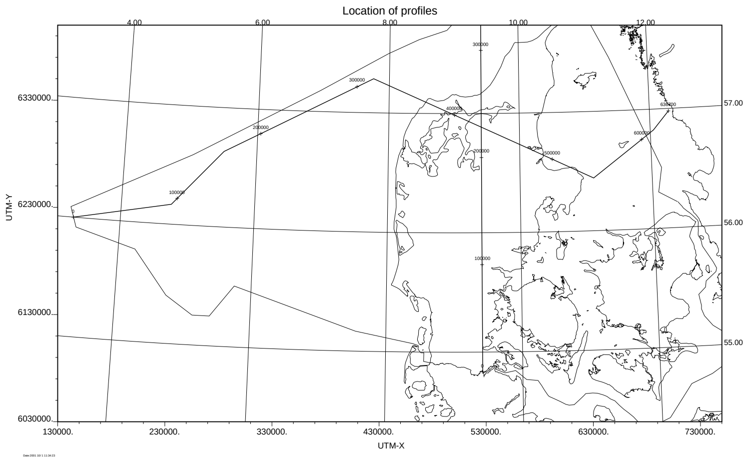

Figure 26: Location of profiles in Figs. 24 and 25

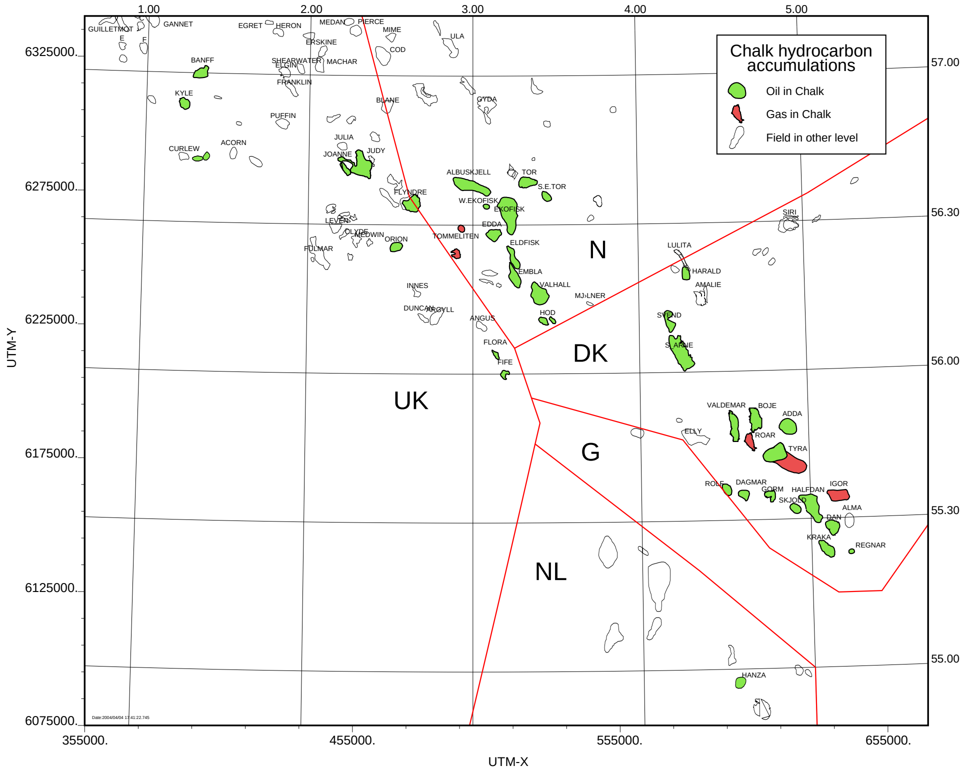

Figure 27: Location of hydrocarbon accumulations in the North Sea with chalk fields highlighted.

7 References

Al-Chalabi, M. 1981: Velocity determination from seismic reflection data. In A. A. Fitch (ed.): Developments in geophysical exploration methods. Applied Science Publishers Ltd. London, pp. 1-68.

Andersen, C., Clausen, C.K., Møller, C., Nygaard, E. and Stouge, S. 1990: Intra-chalk Study, EFP-87: A Multidisciplinary Breakdown. Geological Survey of Denmark. Internal report 49, September.

Anderson, J. K. 1999: The capabilities and challanges of of the seismic method in chalk exploration. In Fleet, A. J. & Boldy, S. A. R. (eds.) Petroleum Geology of Northwest Europe: Proceedings of the 5th conference. The Geological society, London, 939-947.

Baldschuhn, R., Binot, F., Fleig, S. and Kockel, F. (compilers) 2001: Geotektonischer Atlas von Nordwest-Deutschland und dem deutschen Nordsee-Sektor. Geologische Jahrbuch, Reihe A, Heft 153, 88 p. and 3 CD-ROMs.

Best, G., Jaworowsky, K., Jürgens, U., Pokorski, J., Schlüter, H.-U., Sivhed,U., Vejbæk, O.V. an Wagner, R. 2000: Fault zones in the Southern Baltic Sea and their relevance to the input of natural substances into the marine ecosystems. (INPEC). The Baltic. 6th Marine Geological Conference. Hirtshals, Denmark. GEUS, Danish Council of Oceanology and Baltic Marine Geologists. 7-9 March, 2000, Larsen, B.(ed.): Abstracts , 14-15.

Binzer, K. and Stockmarr, J. 1994: Geologisk kort over Danmark, Geological map of Denmark 1:500.000, Pre-Quaternary surface topography of Denmark. Danmarks Geologiske Undersøgelse, Map series no. 44.

Brasher, J. E. and Vagle, K. R. 1996: Influence of lithofacies and diagenesis on Norwegian North Sea reservoirs. American Association of Petroleum Geologists, 80, 746-769.

Britze, P. and Japsen, P. 1991:Geologisk kort over Danmark, Geological map of Denmark 1:400.000, Det danske Bassin, The Danish Basin, Base Chalk and the Chalk Group. Danmarks Geologiske Undersøgelse, Map Series, 29.

Britze, P., Japsen, P. and Andersen, C., 1995: The Danish Central Graben: Top Chalk and the Post Chalk Group. (Two way travel time and depth, and interval velocity), Danmarks Geologiske Undersøgelse, Map Series 47, 1:200,000, 5 p., 3 maps.

Clausen, O. R. and Huuse, M. 1999: The topography of the Top Chalk surface on- and offshore Denmark. Marine and Petroleum Geology 16, 677-691.

Deegan, C. E., and Scull, B. J. 1977: A proposed standard lithostratigraphic nomenclature for Central and Northern North Sea. Report of the institute of geological sciences; no. 77/25 Bulletin of the Norwegian Petroleum Directorate, 1.

Dennis, H. Baillie, J., Holt, T., and Wessel-Berg, D. 1998: Hydrodynamic activity and tilted oil-water contacts in the North Sea. NPF Conference, Haugesund, 14 p.

Erlström, M. 1990: Petrology and deposition of the Lund Sandstone, Upper Cretaceous, southwestern Scania. Sveriges Geologiska Undersökning Series Ca 74, 91 p.

Erlström, M. 1994: Evolution of Cretaceous sedimentation in Scania. Lund Publications in Geology 122, 36 pp.

Erlström, M., Kornfält, K.-A., and Sivhed, U. 2001: Berggrundskartan 2D Tommelilla NO/2E Simrishamn NV. Sveriges geologiska Undersökning, Af 213.

Gemmer, L., Nielsen, S. B., Huuse, M., and Lykke-Andersen, H. 2002: Post-mid-Cretaceous eastern North Sea evolution inferred from 3D thermo-mechanical modelling. Tectonophysics, 350(4), 315-342

Grigelis, A. A. (ed.) 1991: Geology and Geomorphology of the Baltic Sea (in Russian). Lithuanian Geological Institute, Leningrad "Nedra", 419 p.

Hansen, D. L. and Nielsen, S. B. 2002: Does thermal weakening explain basin inversion? - Stochastic modelling of the thermal structure beneath sedimentary basins. Earth and Planetary Science Letters, 198(1-2), 113-127.

Hansen, D. L. and Nielsen, S. B. 2003: Why rifts invert in compression. Tectonophysics 373, 5-24.

Hommel, V. 1996: Structural evolution of the Rønne - Kolobrzeg Graben area. Master Thesis, University of Copenhagen.

Isaksen, D. and Tonstad, V. 1989: A revised Cretaceous and Tertiary lithostratigraphic nomenclature for the Norwegian North Sea. Norwegian Petroleum Directorate Bulletin 5, 59 p.

Japsen, P. 1993. Influence of lithology and neogene uplift on seismic velocities in Denmark: Implications for depth conversion of maps. American Association of Petroleum Geologists Bull. 77(2), 194-211.

Japsen, P. 1994. Retarded compaction due to overpressure deduced from a seismic velocity/depth conversion study in the Danish Central Trough, North SeS Marine and Petroleum Geology, 11(6) 715-733.

Japsen, P. 1998: Regional velocity-depth anomalies, North Sea Chalk; a record of over-pressure and Neogene uplift and erosion. American Association of Petroleum Geologists, Bulletin 82, 2031-2074.

Japsen, P. 1999: Overpressured Cenozoic shale mapped from veloctiy anomalies relative to a baseline for marine shale, North Sea. Petroleum Geoscience, 5, 321-336.

Japsen, P., 2000: Fra kridthav til Vesterhav, Nordsøbassinets udvikling vurderet ud fra seis-miske hastigheder. Geologisk tidskrift (issued by the Danish geological Society), 2, 36 p.

Japsen, P. and Bidstrup, T. 1999: Quantification of late Cenozoic erosion in Denmark based on sonic data and basin modelling. Bulletin of the Geological Society of Denmark 46, 79-99.

Japsen, P., Bidstrup, T., and Lidmar-Bergström, K. 2002: Neogene uplift and erosion of southern Scandinavia induced by the rise of the South Swedish Dome. In: A. G. Doré, J. A. Cartwright, M. S. Stoker, J. P. Turner and N. White: Exhumation of the North Atlantic Margin: Timing, Mechanisms and Implication for petroleum exploration. Geological Society of London, Spec. Publ. 196, 183 - 207.

Jaritz, W., Best, G., Hildebrand, G. and Jürgens, U. 1991: Regionale Analyse der seismischen Geschwindigkeite in Nordwestdeutschland. Geologisches Jahrsbuch, Reihe E, 45, 23-57.

Jensen, S. K. 1998: Structural development of the Sorgenfrei - Tornquist Zone and adjacent areas, Norwegian North Sea Sector. Master Thesis, Aarhus University.

Johnson, H. and Lott, G. K. 1993: Cretaceous of the Central and Northern North Sea. Knox, R. W. O'B. and Cordey, W. G. (eds.): Lithostratigraphic nomenclature of the UK North Sea, Vol. 2, Britich geological Survey, (Nottingham).

Kramarskiej, R. (ed.) 1999: Geological map of the Baltic Sea Bottom without Quaternary deposits. 1: 500 000. Panstwowy Instytut Geologiczny. Gdansk - Warszawa.

Kumpas, M. G.1980: Seismic Stratigraphy and Tectonics in the Han bay. Stockholm Contribution in Geology 34 (4), 35-168.

Køgler, F.-C. and Larsen, B. 1979: The west Bornholm basin in the Baltic Sea: geological structure and Quaternary sediments. Boreas. vol. 8, pp 1-22. Olso.

Lemke W. 2000: Sedimentation und paläogeographische entwicklung im westlichen Ostseeraum (Mecklenburger Bucht bis Arkona Becken) vom Ende der Weichselvereisung bis zur Litorinatransgression, Habilitationsschrift zur Erlangung des akademischen Grades doctor rerum naturalium habilitatis (Dr. rer. nat. habil.) an dr Mathematisch - Naturwissenschaftlichen Fakultät der Ernst Moritz-Arndt Universität Greifswald.

Megson, J. B. and Hardman, R. 2001: Exploration for and development of hydrocarbons in the Chalk of the North Sea: a low permability system. Petroleum Geoscience, 7, 3-12.

Mogensen, T. E. 1995: Triassic and Jurassic structural development along the Tornquist Zone, Denmark. Tectonophysics 252, 197-220.

Mogensen, T. E. and Jensen, L. N. 1994: Cretaceous subsidence and inversion along the Tornquist Zone from Kattegat to the Egersund Basin. First Break, 12(4) April, 211-222.

Moss, B., Barson, D., Rakhit, K., Dennis, H. and Swarbrick, R. 2003: Formation pore pressures and formation waters. In Evans, D., Graham, C., Armour, A. and Bathurst, P. (eds.): The Millennium Atlas: Petroleum geology of the central and northern North Sea. Geological Society of London, 317-329.

NGU (Norges Geologiske Undersøkelse) Rapport 96.138:

NLFB-GGA 1996: Erdöl und Erdgas in der Bundesrepublik Deutschland 1996. Niedersächsisches Landesamt für Bodenforschung, Hannover, 51p.

Rasmussen, E. S., Vejbæk, O. V., Bidstrup, T., Piasecki, S and Dybkjær, K. (in press): Late Cenozoic depositional history of the Danish North Sea Basin: implications for the petroleum systems in the Kraka, Halfdan, Siri and Nini fields. 6^{th} *Petroleum Geology Conference, London.*

Rempel, H. 1992: Erdölgeologische Bewertung der Arbeiten der Gemeinsamen Organisation Petrobaltic in deutschen Schelfbereich. Geologisches Jahrbuch, Reihe D, H 99, Hannover, 32 p.

Schlüter, H. U., Jürgens, U., Best, G,. and Binot, B. 1997: The "Structural Atlas of the Southern Baltic Sea" (SASO) Project; first results. In Cato, I. Klingberg, F. (eds): Proceedings of the fourthMarine geological conference; "The Baltic". Sveriges Geologiska Undersökning. Series Ca. 86, 159-163. Uppsala.

Seifert, T. and Kayser, B. 1995: A High resolution spherical grid topography of the Baltic Sea. Meereswissensachaftliche Berichte, Marine Science Reports No. 9. Institut für Ostseeforschung, Warnemünde, 89 p.

Sivhed, U., Wikman, H. and Erlström, M. 1999: Beskrivning till berggrundskartorna 1C Trelleborg NV och SO samt 2C Malmö SV, SO, NV och NO. Sveriges Geologiska Undersökning Serie Af 191, 192, 193, 194, 196, 198. 143 p.

Stenestad, E. 1976: Københavnsområdets geologi, især baseret påcitybane undersøgelserne. Danmarks Geologiske Undersøgelse,III, 45, 149 p.

Surlyk, F. 1982: Upper Cretaceous and Danian outcrops in Scania and East Denmark. In The Upper Cretaceous and Danian of NW Europe. Excursions : 069A. 26th International geological Congress, Paris 1980, 31-62.

Surlyk, F., Dons, T., Clausen, C. K., and Higham, J. 2003: Upper Cretaceous. In Evans, D., Graham, C., Armour, A. and Bathurst, P. (eds.): The Millennium Atlas: Petroleum geology of the central and northern North Sea. Geological Society of London, 213-233.

Ter-Borch, N. 1991: Geologisk kort over Danmark, Geological map of Denmark 1:500.000, Structural map of the Top Chalk Group. Danmarks Geologiske Undersøgelse, Mapseries no. 7.

Thomasen, J. B. and Jacobsen, N. L. 1994: Dipping fluid contacts in the Kraka Field, Danish North Sea. SPE 28435, 763-772.

Vejbæk, O. V. 1997: Dybe strukturer i danske sedimentære bassiner. Geologisk Tidskrift, 4, 1-31.

Vejbæk, O. V. and Andersen, C. 1987: Cretaceous Early Tertiary inversion tectonism in the Danish Central Trough. - Tectonophysics, vol. 137, pp. 221 - 238.

Vejbæk, O. V. and Andersen, C. 2002: Post Mid-Cretaceous Inversion Tectonics in the Danish Central Graben - regionally synchronous tectonic events? Bulletin of the Geological Society of Denmark, 49, 139-144.

Vejbæk, O. V. and Britze, P. (eds.) 1995: Top pre-Zechstein, Geological Map of Denmark 1:750000 Danmarks Geologiske Undersøgelse, Map series 45, 9p., 3 maps, 3 enclosures.

Vejbæk, O. V., Stouge, S. and Damtoft Poulsen, K. 1994: Palaeozoic tectonic and sedimentary evolution and hydrocarbon prospectivity in the Bornholm area. Danmarks geologiske Undersøgelse, Ser. A(34), 23pp. 4 plates.

Vejbæk, O. V., Frykman, P., Bech, N. and Nielsen, C. M. in press: The history of hydrocarbon filling of Danish chalk fields. 6^{th} *Petroleum Geology Conference, London.*

Vindum, J. 2002: Upper Cretaceous and Danian deposits illustrated by seismic interpretation in relation to Djursland and Kattegat, East Denmark. Master Thesis, University of Copenhagen.

Ziegler, P. A. 1995: Dynamics of intra-plate compressional deformation: the Alpine foreland and other examples. Tectonophysics 252, 7-59.

8 Appendix

This mapping project applies the Universal Transversal Mercator (UTM) projection in zone 32 (central meridian 9°E) using the Hayford 1909 ellipsoid. Other projection types were, however, encountered during map compilation. To give an indication on how these were treated, brief descriptions are given below. They include: Gauss-Krüger, Mercator and "Rikets Nät" projections. In a few cases only a change of ellipsoid and/or a change of central meridian was required. By keeping track of what ellipsoid has been in use, a mathematically derived positioning error in the order 250-300 m can be avoided. Datum changes have not been considered which may introduce mathematically derived positioning errors that may approach 10 m in the worst cases. This is considered far below drafting precision (original, and during reproduction) and digitization errors. Drafting and digitization errors are therefore the most likely positioning errors in the resulting maps.

8.1 Gauss-Krüger projection

This projection is a transversal mercator similar to the UTM projection, but without the central meridian scaling factor (=1). Therefore projection distortion increases from the central meridian which is remedied by applying narrower projection zones. This projection type is typically applied in the German sector based on the Bessel 1841 ellipsoid. A fortran program has been used for converting these maps to geo-koordinates. Then an ellipsoid shift is performed followed by conversion into the UTM projection of this project.

8.2 "Rikets Nät" projection

This projection is applied in Sweden and is a special version of the Gauss-Krüger projection. It also applies the Bessel 1841 ellipsoid (Semi Major Axis = 6377397.155m and Inverse Flattening (1/f) 299.1528128). The central meridian is 15°48'29".8 or 15.808278° (passing through the old observatory near Stockholm) and latitude of origin is 0°. False northing is 0 m and false easting is 1500 000 m (or 1 Mm larger than UTM false easting).

See also `http://www.lm.se/geodesi/refsys/rt/projektioner_i_rt.htm`.

8.3 Mercator projection

In this projection digitization may be performed directly as geokoordinates. Longitude values vary linearly, but latitude values vary non linearly. Digitization is performed assuming bi-linear axis. Following digitization a fortran program is applied that corrects for the actual non-linear latitudinal spacing. The resulting corrected geo-coordinates may be transferred to the Hayford 1909 ellipsoid and subsequently transformed into UTM coordinates. Since basic data for these maps typically are positioned using GPS that refers to the WGS-84 ellipsoid, an ellipsoid change must be applied to maintain sufficient accuracy.

9 Enclosures

Enclosure 1: Top Chalk Depth structure map in scale 1:1,170,000.

Enclosure 2: Base Chalk Depth structure map in scale 1:1,170,000.

Enclosure 3: Chalk Group isopach map in scale 1:1,170,000.

Top Chalk depth structure map; Ultimo 2003

Enclosure 1

G E U S
Report file no.
Enclosure
25385 (01/03)

Base Chalk Depth structure map; Ultimo 2003

Enclosure 2

GEUS
Report file no.
Enclosure
25385 (02/03)

Chalk Group isopach map

Enclosure 3